CMB Physics: The Next Generation

David Spergel

Where do we go from here?

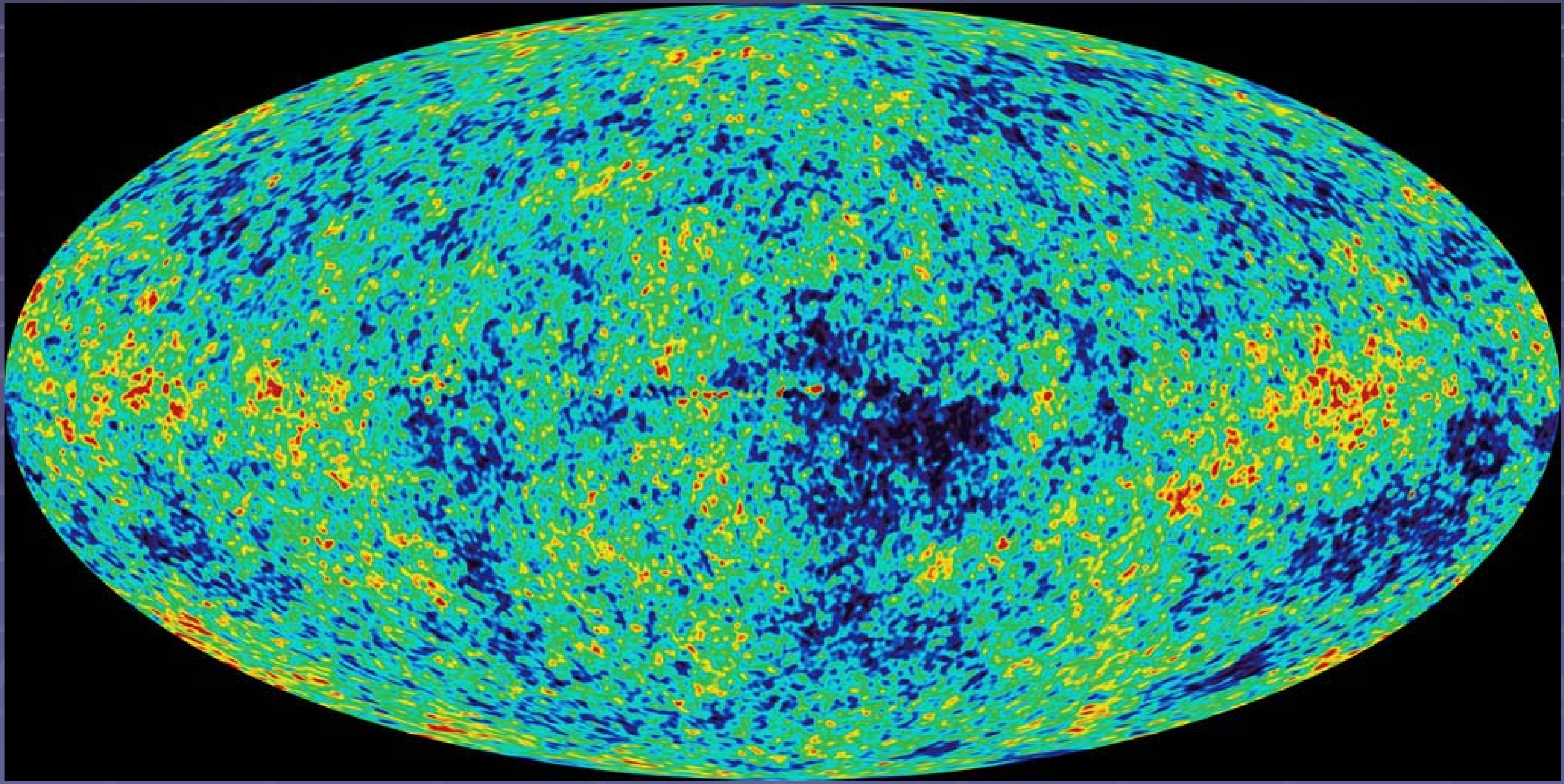

Current Power Spectrum Data

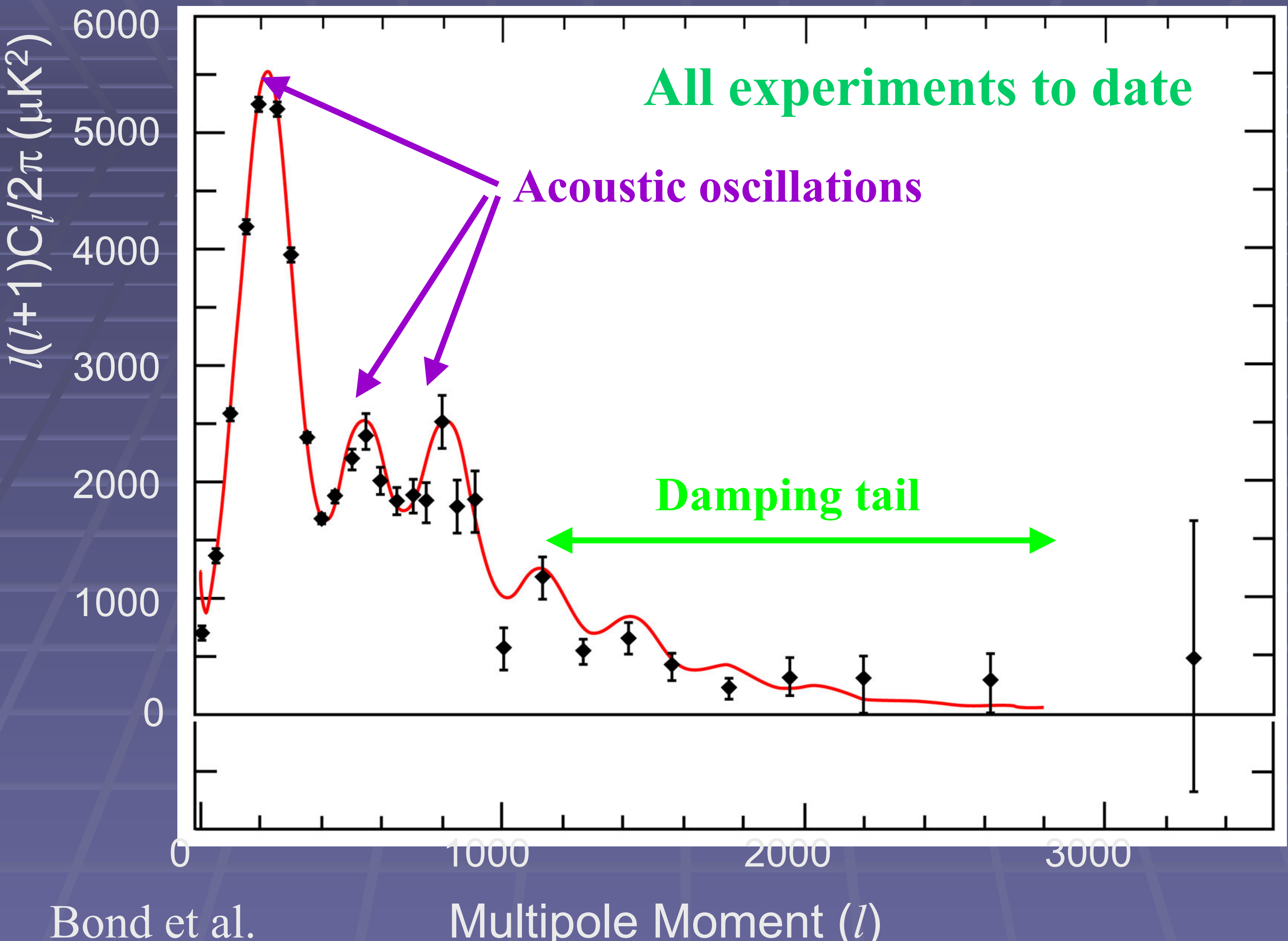

Bond et al.

The Next Decade

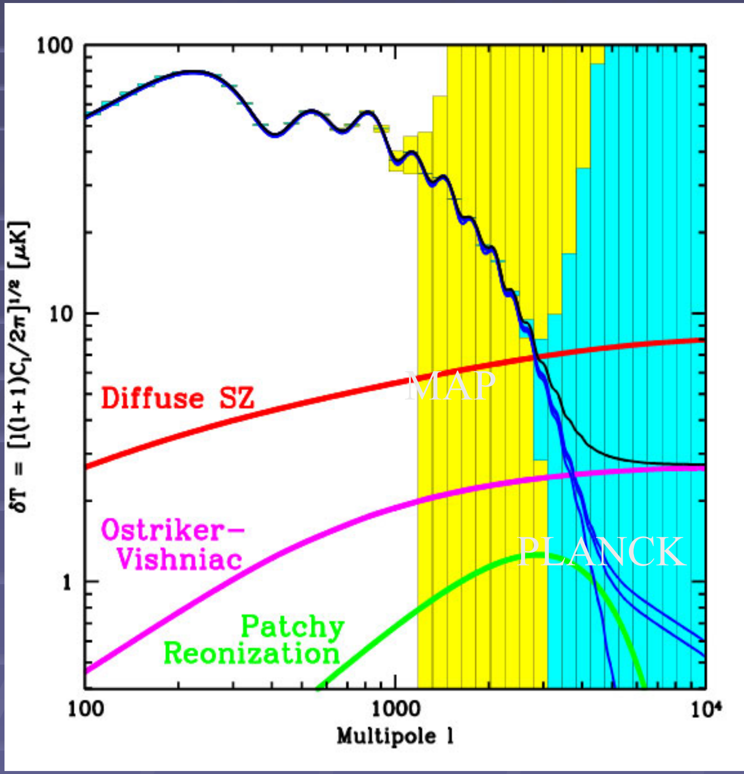

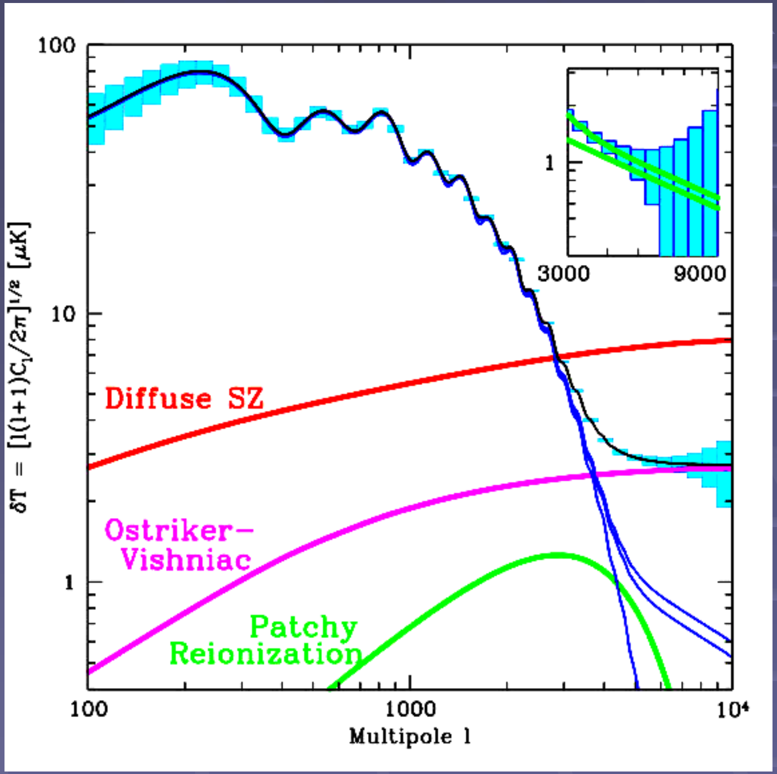

Higher Resolution,….

WMAP 4 + ACT+ QUEST + BICEP

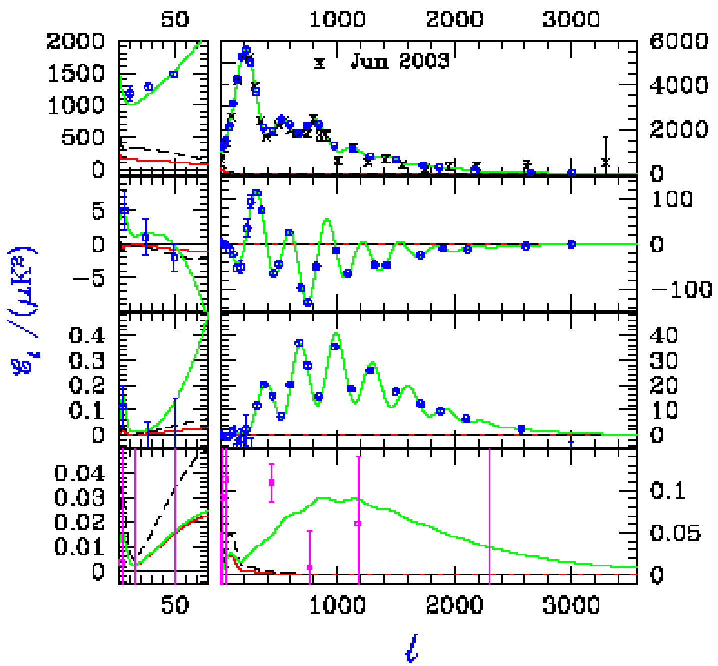

Figure 5: Forecast for how well a high-resolution ground-based polarization-sensitive large-array experiment like ACT or SPT can do, in conjunction with WMAP4. The specific assumptions used are given in the caption of Fig. 10 and are conservative over what might be achievable from the ground using bolometer arrays. There is a trade off of sky coverage and noise. ($f_{sky} = 0.024$ here, with larger and shallower often improving cosmic parameter determinations, and smaller and deeper making the lens-induced B-modes potentially detectable.) Apart from the current DASI, WMAP, Boomerang and CBI data already in to flesh out the EE spectrum, a number of other experiments are planned. These include some in the very near future, e.g., QUaD and BICEP. Forecasts for the proposed QUIET with HEMT arrays look as promising as those for polarized ACT/SPT. Given the expected signal levels, all ground and space CMB information available will be needed and used to get clean primary polarization results.

Planck

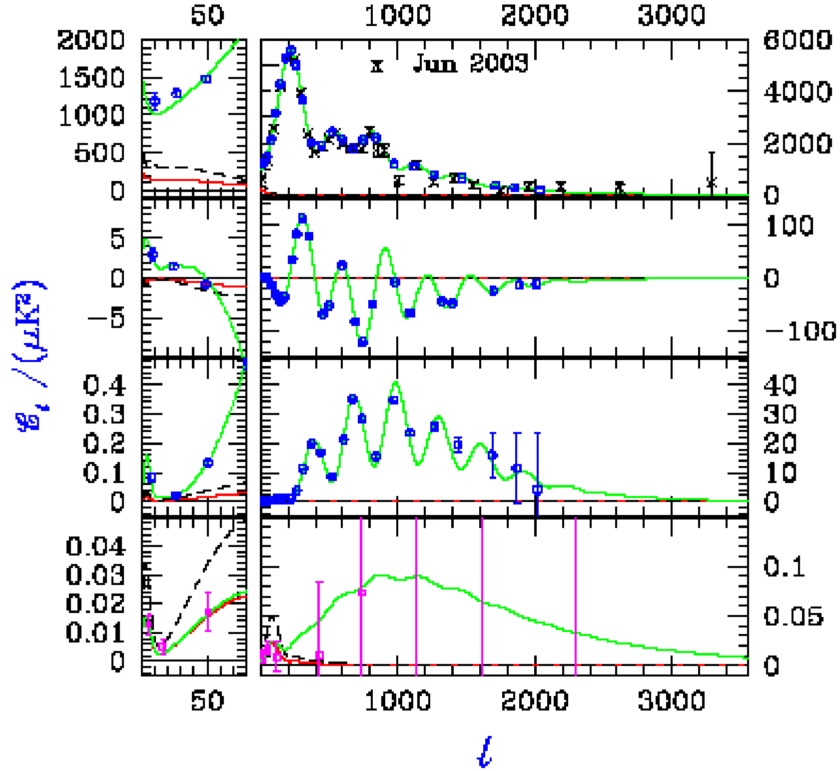

Figure 4: Forecast for how well Planck can do with just its 150 GHz channels for one year of data, quite a conservative estimate. Even so, note the anticipated detection level of EE and TE at low ℓ, sharpening the τ_C determination, and the possibility of a statistically significant direct tensor-induced B-mode detection. Although ground-based experiments at high resolution should have a huge pre-Planck impact (e.g., Fig. 5), the all-sky nature of Planck, its large set of polarization-sensitive frequencies and likely longer observing time than that assumed here will make it extremely powerful to sort out the many signals that complicate the "primary" quest.

Bond et al. 0406195

Parameter Limits Improve

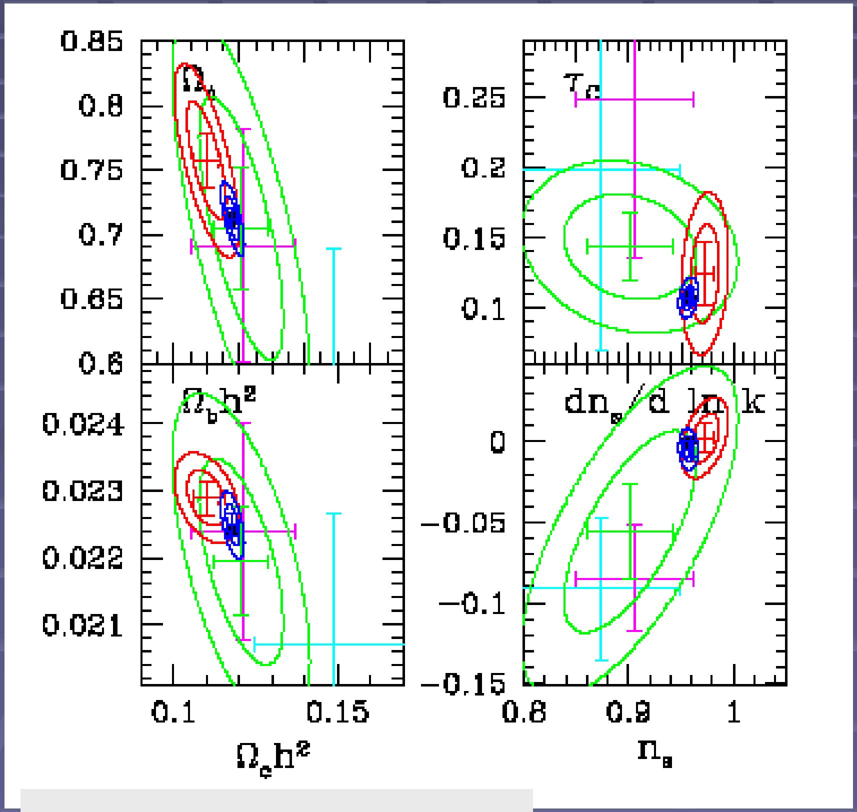

WMAP 1

WMAP 4

WMAP 4 + ACT

Planck

- Pin down slope and spectral index
- Reionization properties
- Assist in dark energy constraints
  - $\Omega_m h^2$
  - Angular diameter distance
  - Normalization of amplitude of fluctuations

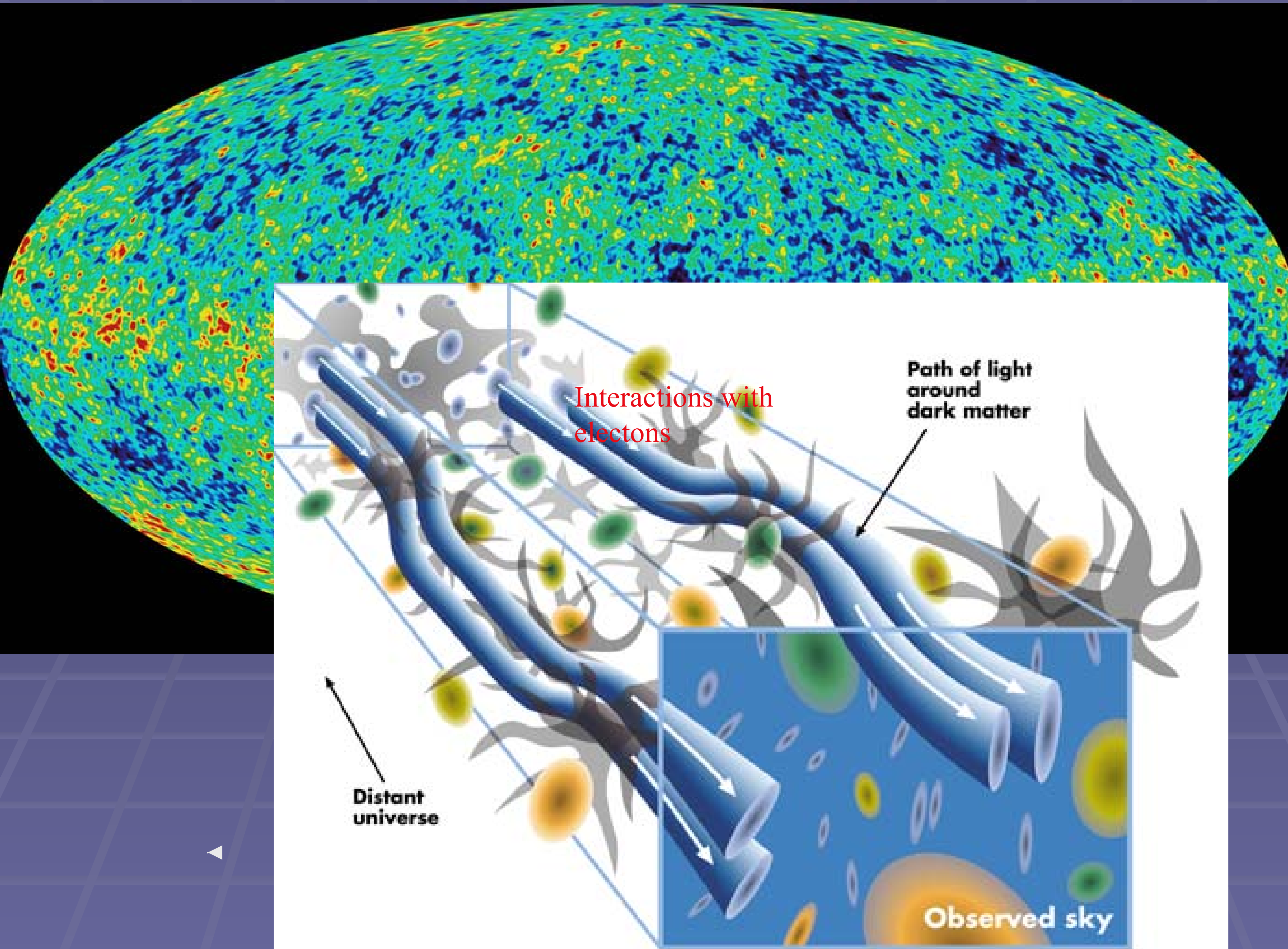
Interactions with
electons
Path of light
around
dark matter
Distant
universe
Observed sky

Reionized Gas Layer

$$\frac{\delta T}{T} = \int d\eta\, n_e^0 [1 + \delta(\eta))] v(\eta) \sigma_T c$$

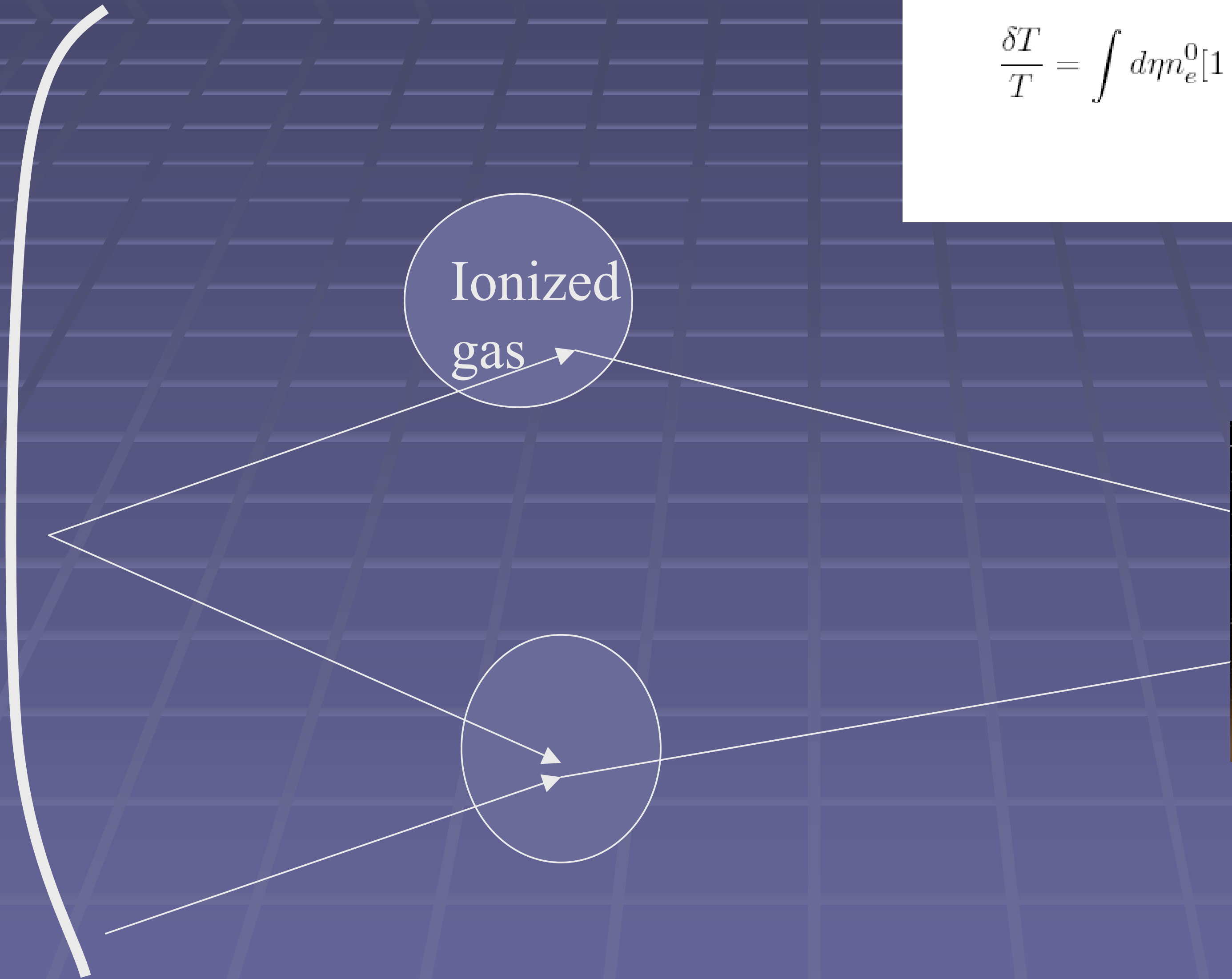

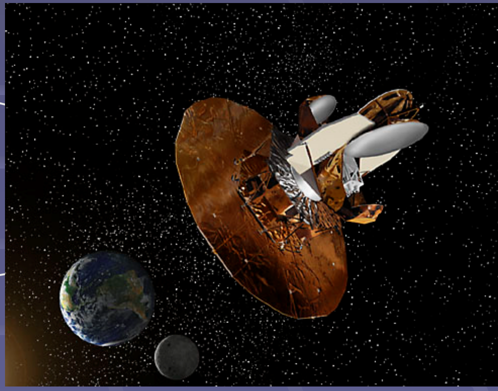

Scattering erases small scale temperature fluctuations

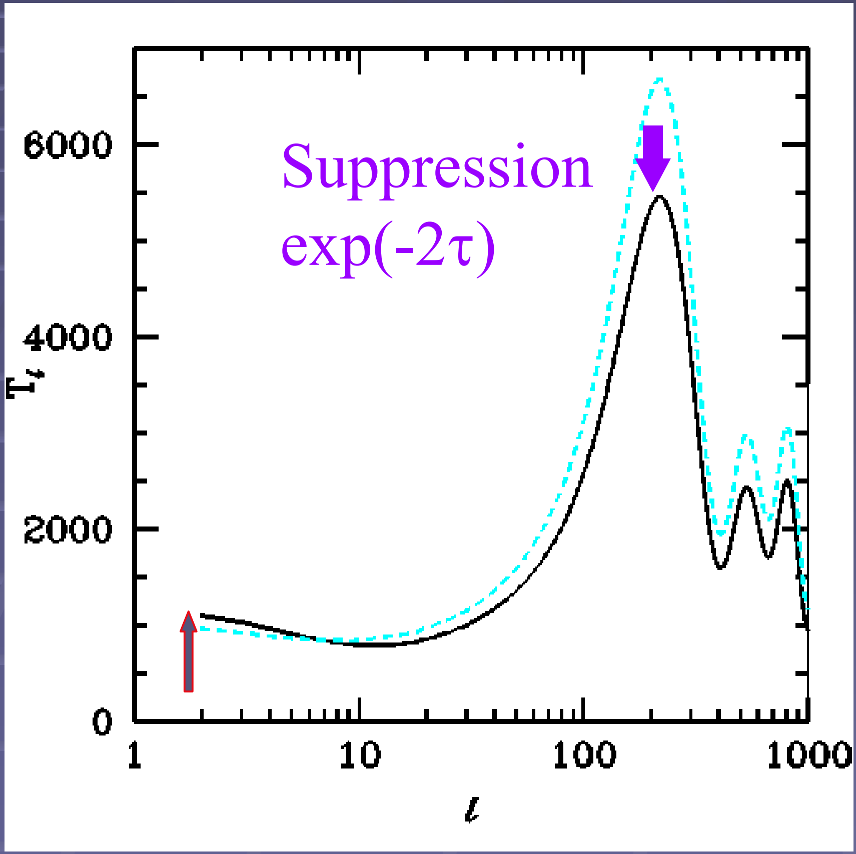

Mixing erase fluctuations

Large scale flows enhance fluctuations

Degeneracy between fluctuation slope and τ

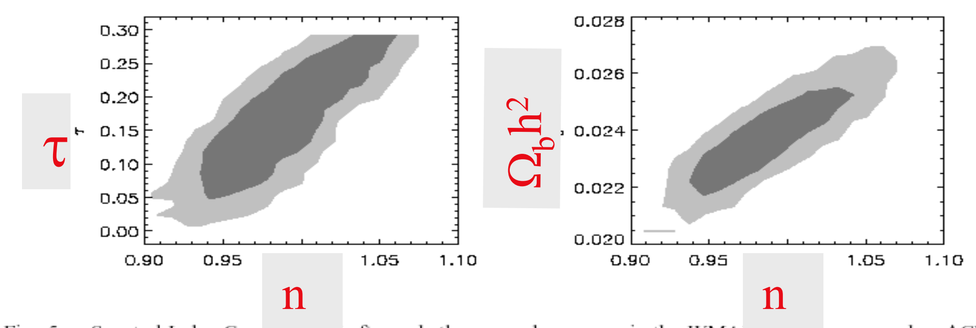

Fig. 5.— Spectral Index Constraints. Left panel: the $n_s - \tau$ degeneracy in the *WMAP* data for a power-law ΛCDM model. The TE observations constrain the value of τ and the shape of the C_l^{TT} spectrum constrain a combination of n_s and τ. Right panel: $n_s - \Omega_b h^2$ degeneracy. The shaded regions show the joint one and two sigma confidence regions.

- Strongest degeneracy in one year data
- Most dramatic improvement with more data

Large Angle Polarization Fluctuations

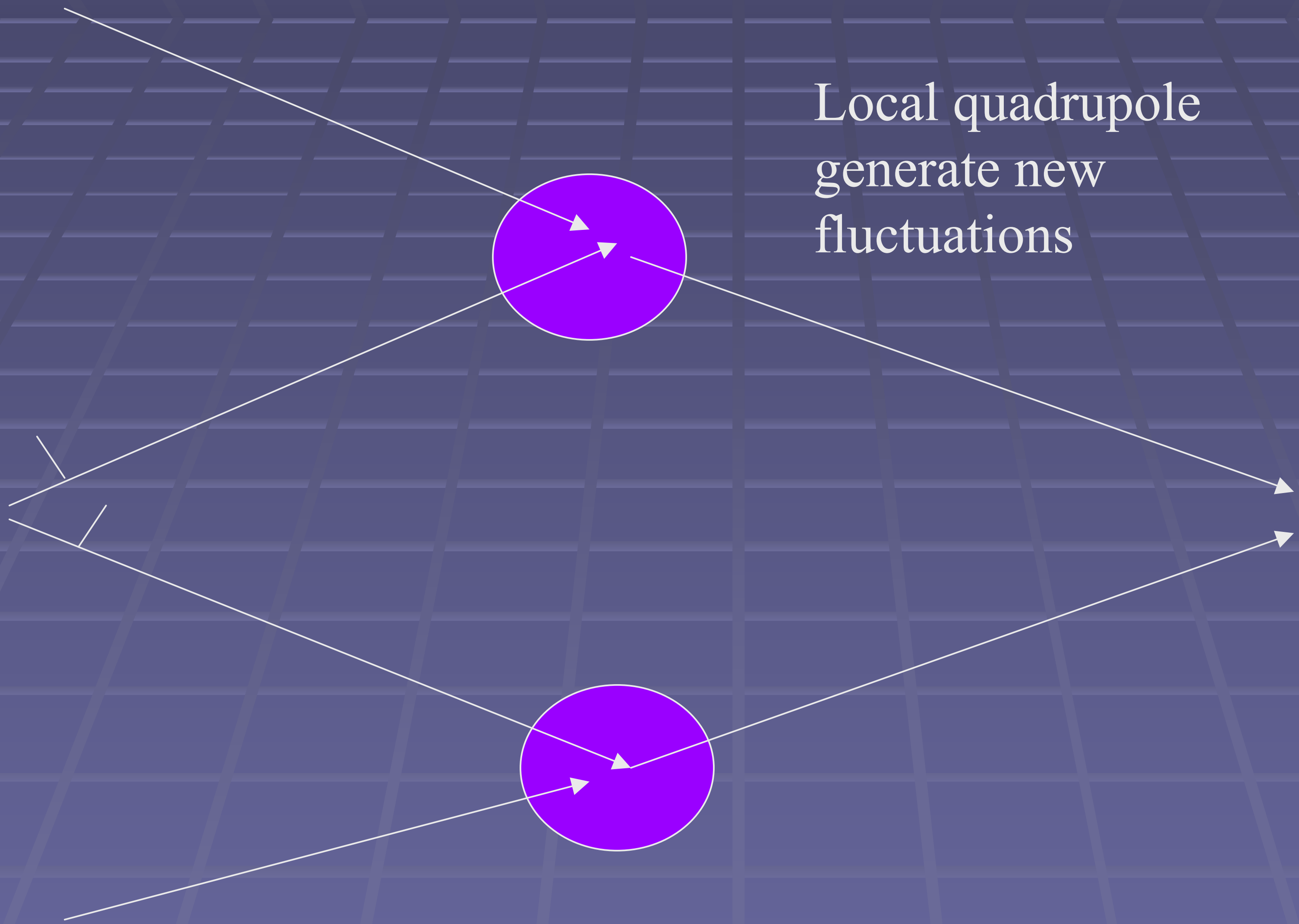

Local quadrupole generate new fluctuations

CMB Polarization

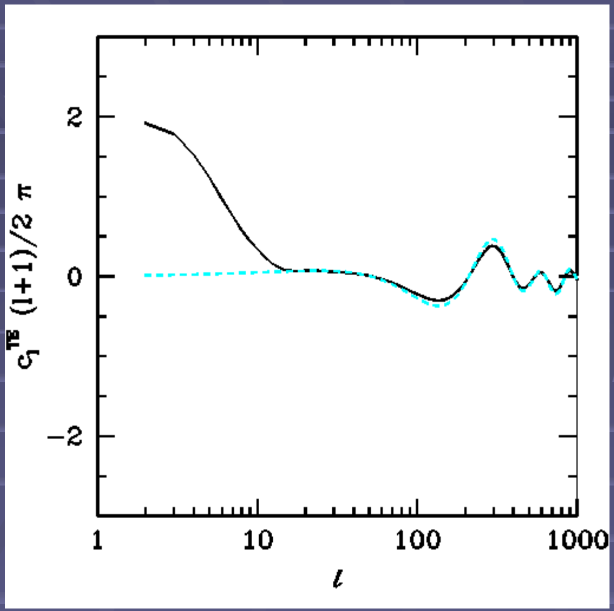

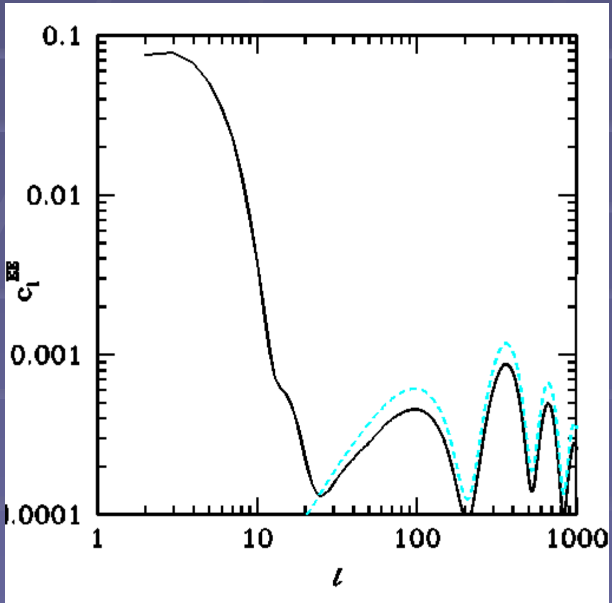

- CMB polarization can be split into two pieces: E and B
- Scalar fluctuations Generates TE and EE signal
- Gravity waves generate TE, EE and BB signal

EE Polarization Signal

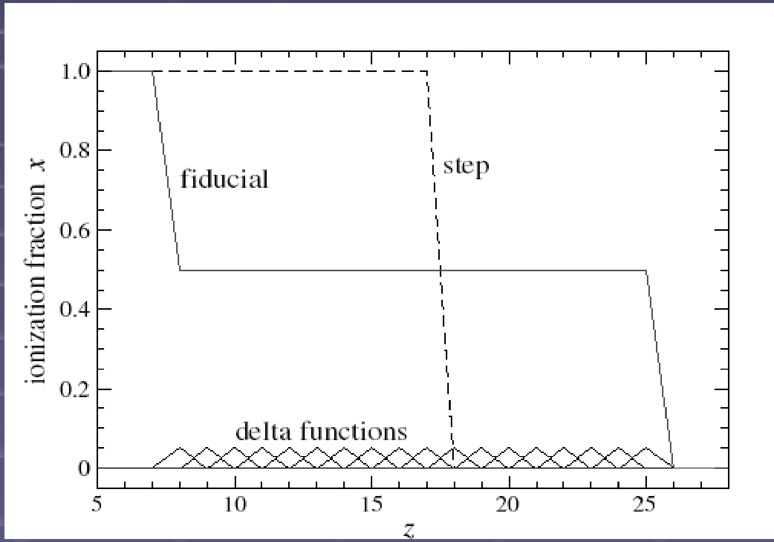

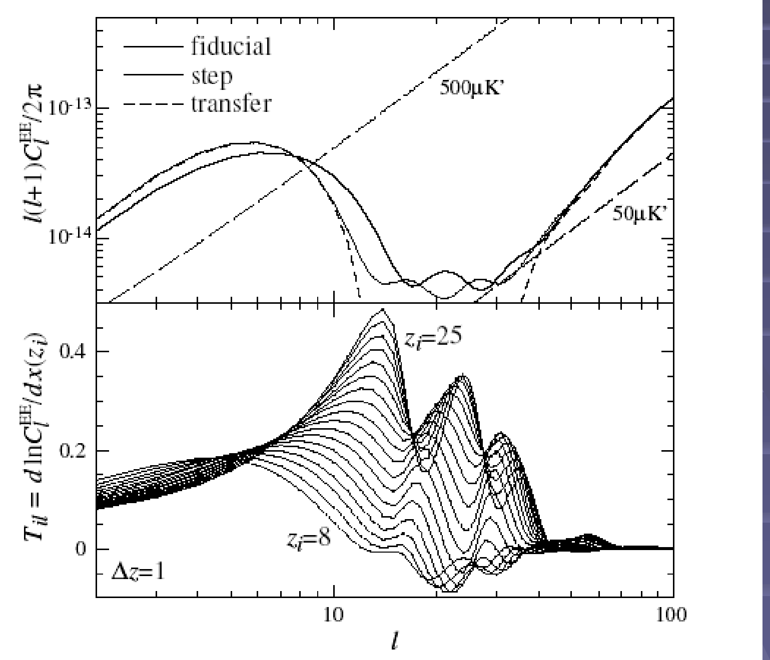

FIG. 2: Top: E-mode polarization power spectrum for: the fiducial model of Fig. 1 (thick); the step function model (thin); the step function model with deviations transferred onto the fiducial model (dashed); instrumental noise $w_P^{-1/2}$ (denoted in μK-arcmin) that roughly brackets expectations from WMAP and Planck (long dashed). Bottom: the transfer function or fractional power spectrum response to a delta function perturbation of unit amplitude at $8 \leq z_i \leq 25$.

- Amplitude and peak position sensitive to reionization history

Holder & Hu 2003

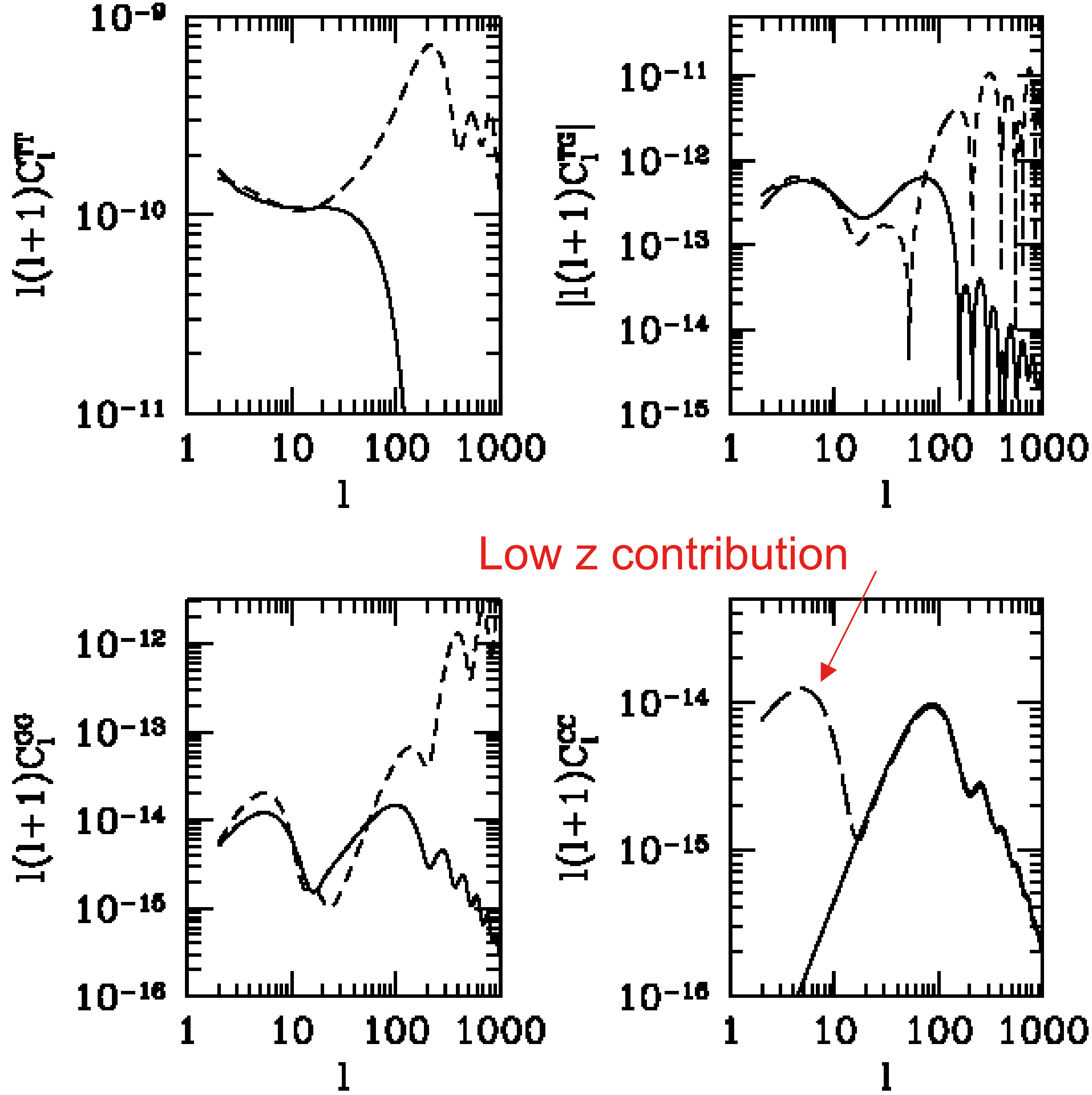

$l(l+1)C_l^{TT}$
$|l(l+1)C_l^{TG}|$
$l(l+1)C_l^{GG}$
$l(l+1)C_l^{CC}$
10^{-9}
10^{-10}
10^{-11}
10^{-12}
10^{-13}
10^{-14}
10^{-15}
10^{-16}
1
10
100
1000
l
Low z contribution

Current Status

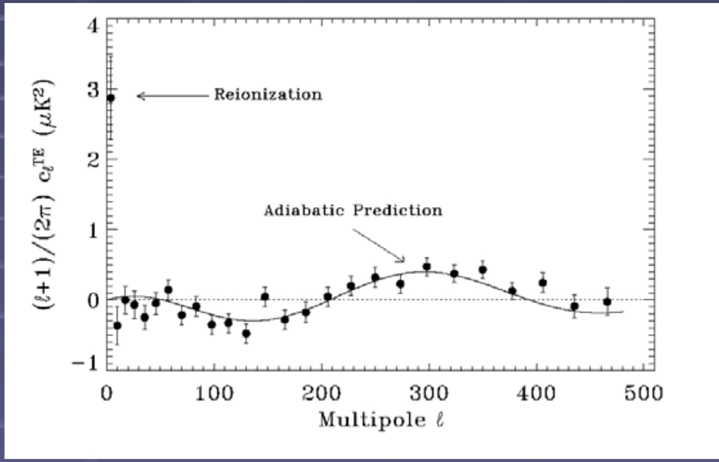

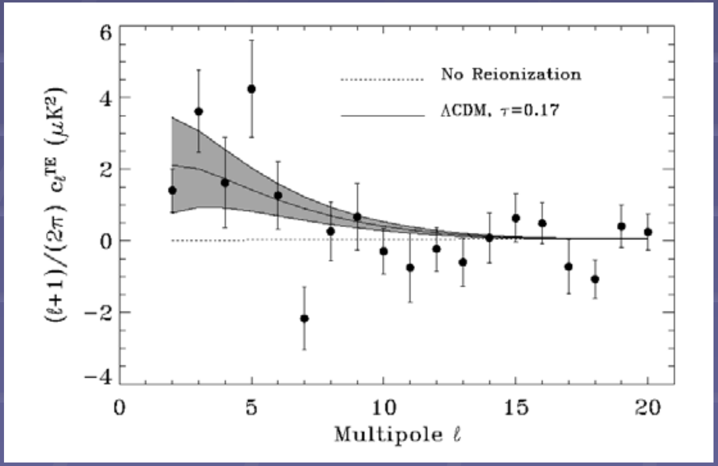

- Weak signal
  - signal is statistical rather than a detection in each pixel
- Foregrounds
  - Synchrotron (dominant)
  - Dust
- Systematic Uncertainties
- Significant uncertainty in reionization redshift
  - Will improve with more data
  - Polarization auto-correlation
  - $\Delta\tau/\tau$~0.1 in 4 year data

Cosmic Timeline for Small Scale CMB Science

- First galaxies
- Universe is reionized
- Ostriker-Vishniac/KSZ

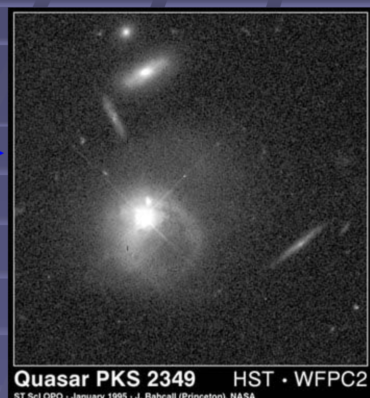

- Surveys of Sunyaev-Zel'dovich (SZ) clusters
- Diffuse thermal SZ

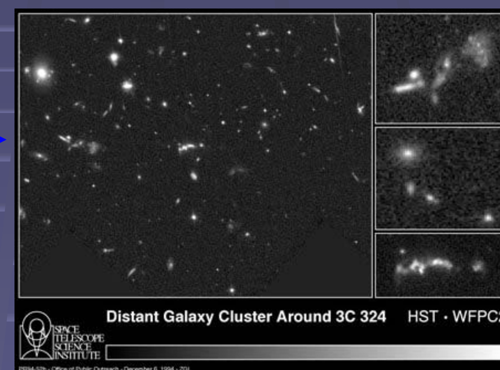

- Extraction of cosmological parameters

- Initial conditions for structure formation

- N(mass,z) – Evolution of Cosmic Structure
- Lensing of the CMB
- The growth of structure is sensitive to w and m_n
- Additional cross-checks from correlations among effects

z = 1000
t = 4 x 10^4 yrs

z = 7
t = 3 x 10^6 yrs

z = 1
t = 1 x 10^9 yrs

z = .25
t = 12 x 10^9 yrs

now

Primary CMB | CMB Lensing | OV/KSZ | Diffuse Thermal SZ | Cluster Surveys

Gravitational Lensing of CMB

- Photons paths are deflected by mass fluctuations
  - Hot spots (and cold spots) behind a cluster are smaller and are stretched

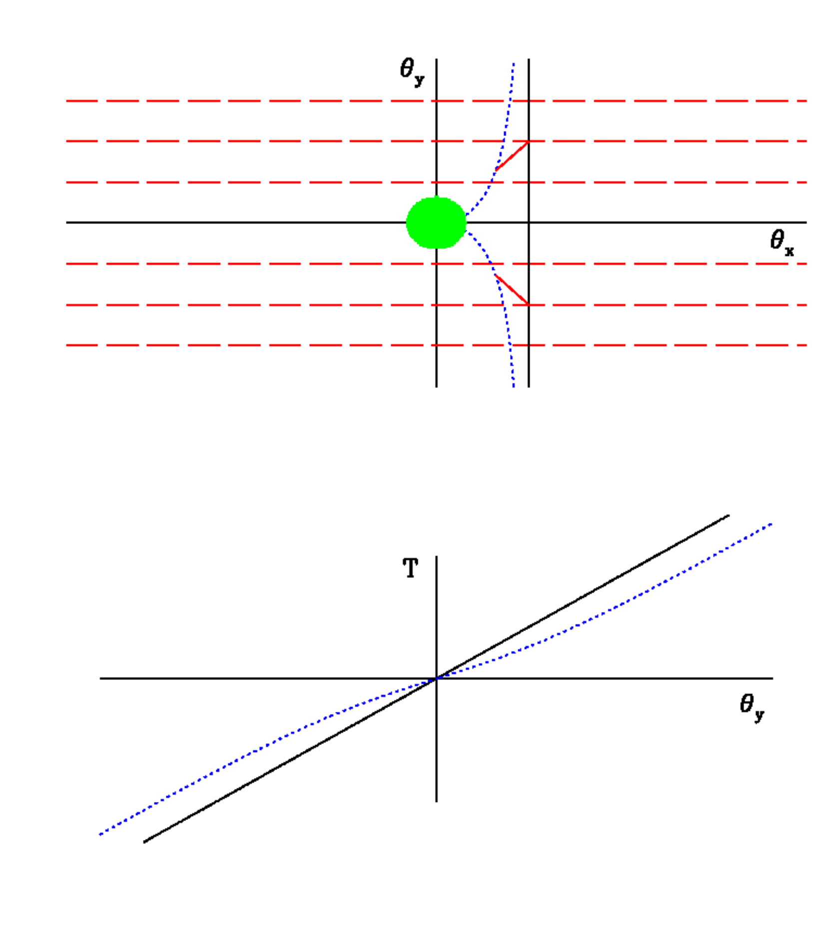

$$T(\boldsymbol{\theta}) = \tilde{T}(\boldsymbol{\theta} + \delta\boldsymbol{\theta})$$
$$\approx \tilde{T}(\boldsymbol{\theta}) + \delta\boldsymbol{\theta} \cdot \nabla\tilde{T}(\boldsymbol{\theta}) + \frac{1}{2}\delta\theta_i\delta\theta_j\partial_{ij}\tilde{T}(\boldsymbol{\theta}).$$

Power Spectrum

- Acoustic peaks are smeared out
- Additional power on small angular scales
- Lensing signal should correlate with galaxy distribution (just as galaxy lensing-galaxy)

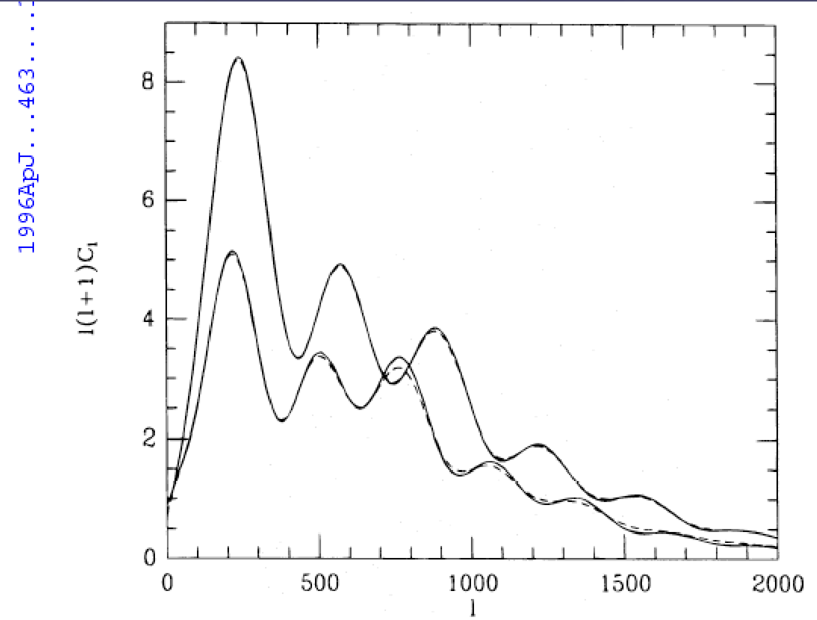

FIG. 2.—CMB anisotropy power spectrum $l(l+1)C_l$ vs. l with lensing (*dashed lines*) and without lensing (*solid lines*). Upper curves are for adiabatic CDM model with $h = 0.5$, $\Omega_{m0} = 0.4$, and $\Omega_{v0} = 0.6$, lower curves are for adiabatic CDM model with $h = 0.5$, $\Omega_{m0} = 1$ and $\Omega_{v0} = 0$. Both models are normalized to *COBE*. Lensing smoothes the sharp features in the power spectrum but leaves the overall shape unchanged. The two models show a typical range of the lensing effect on CMB.

Seljak 1996

Generation of New Fluctuations

- E modes are distorted into B modes on small scales
  - Lensing rotates polarization vectors
- Non-Gaussian fluctuations are generated on small scales (non-trivial 4 point function)

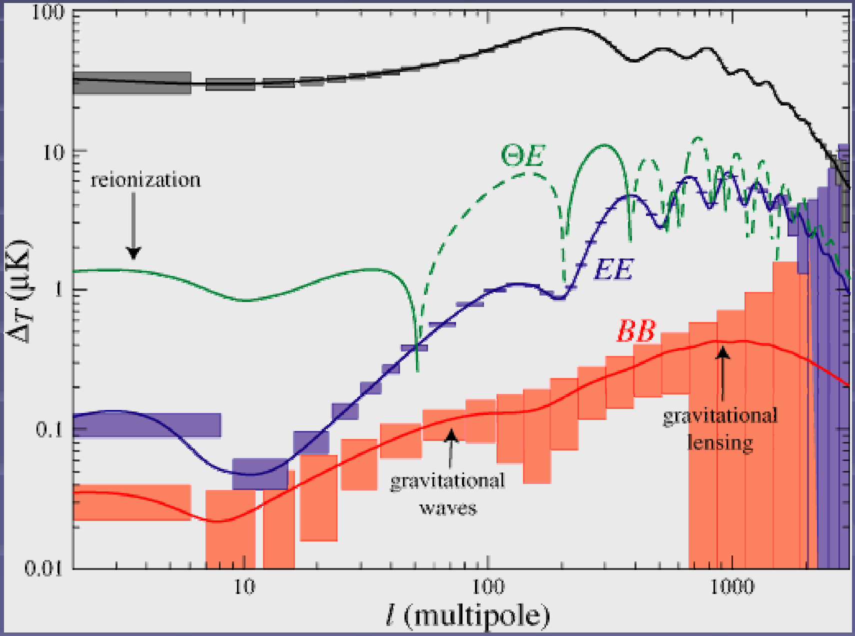

Hu and Dodelson (2002)

Measuring Shear Power Spectrum

- CMB lensing is more sensitive on large angular scales
- Very promising to combine lensing seen by Planck with lensing seen by LSST
  - Independent systematics
  - Multiple lens sheets
- Small scale surveys and ACT

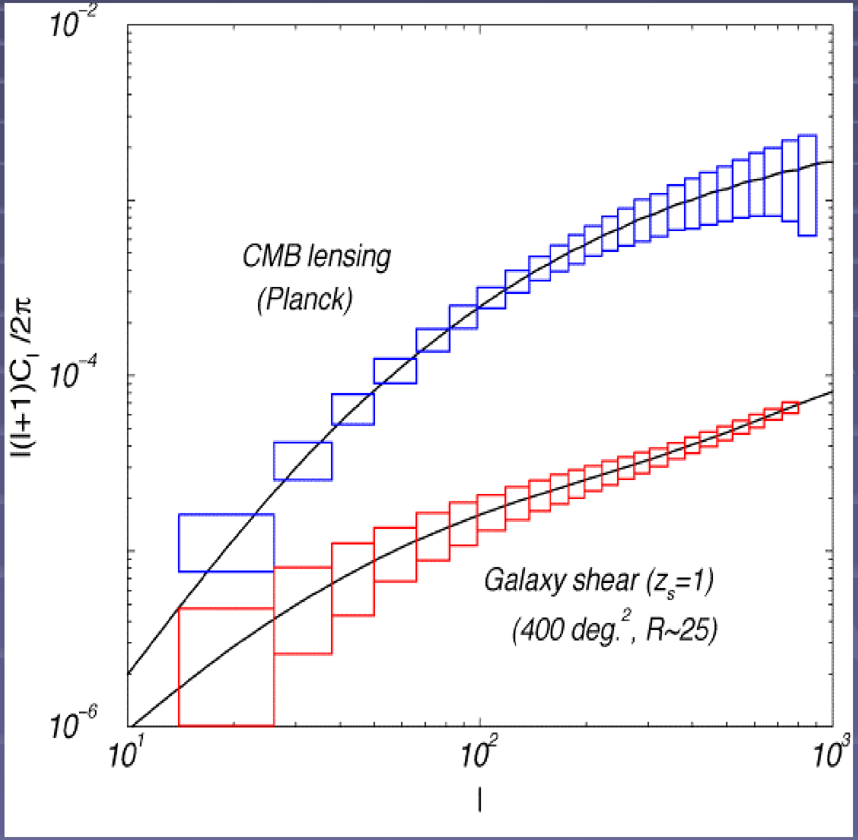

Cooray
2002

Lensing of the CMB

• Lensing arises from integrated mass fluctuations along the line of sight.

• The CMB acts as a fixed distance source, removing the degeneracy inherent to other lensing measurements.

• Signal at $l = 1000\text{-}3000$

• Image distortion – only a minor effect in the power spectrum.

• *Must* have a deep, high fidelity map to detect this effect.

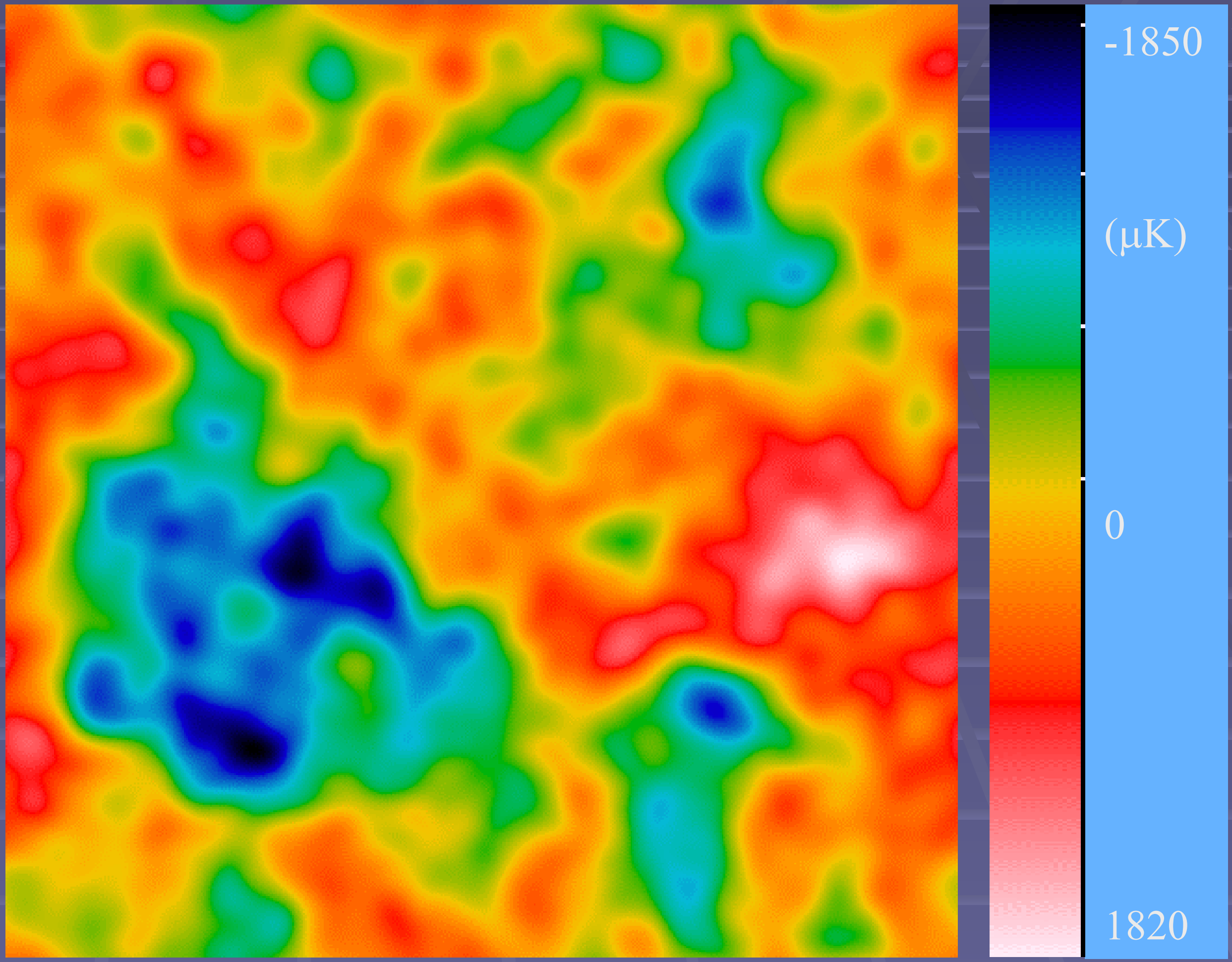

CMB

1.4°x 1.4°

Lensing of the CMB

- RMS signal well above noise floor.
- Isolate from SZ and point sources spectrally.
- Identify with distinctive 4-point function.

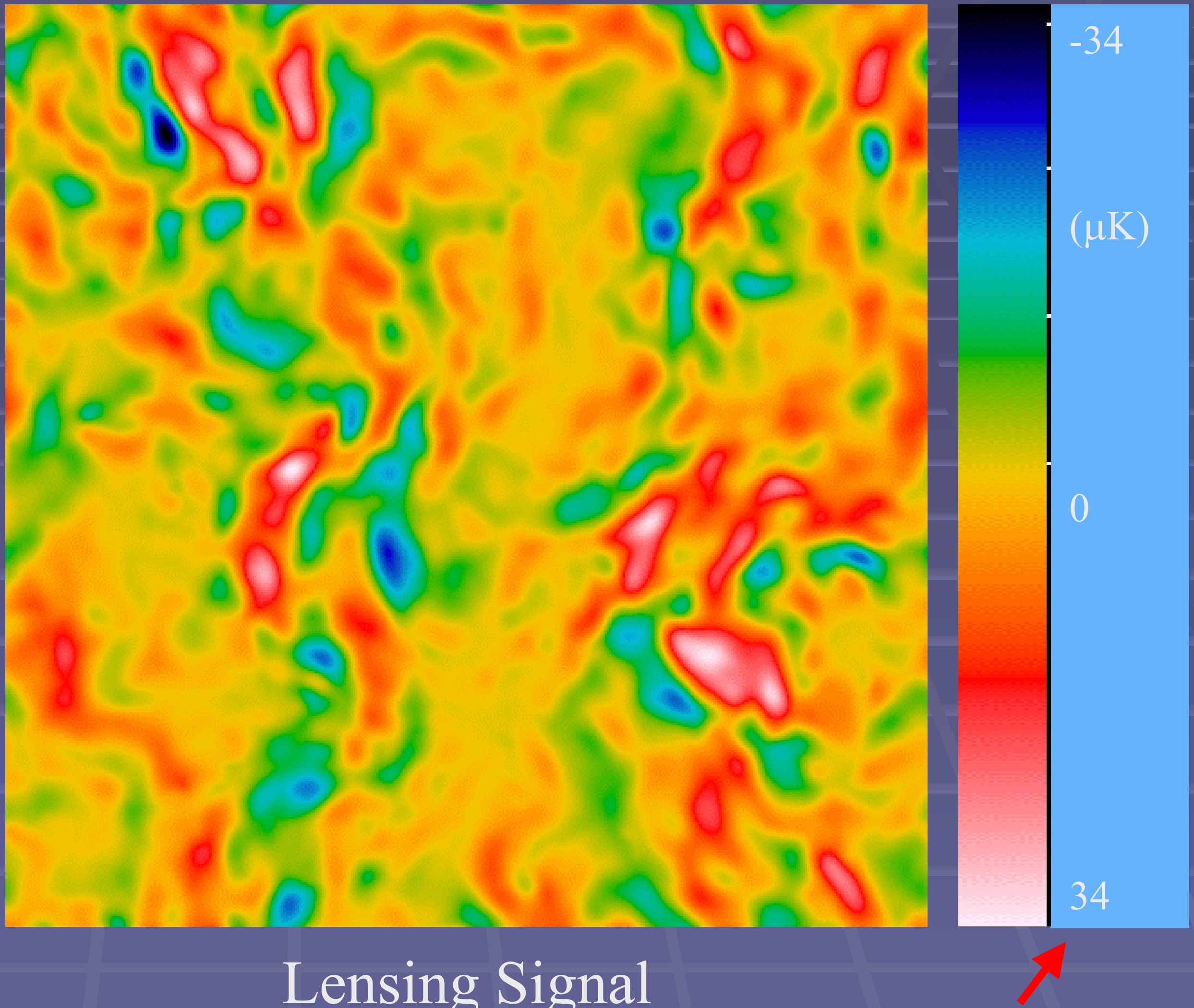

Lensing Signal

1.4°x 1.4°

Sunyaev-Zeldovich Effect

$$y = \frac{\sigma_T c}{m_e c^2} \int d\eta n_e(\eta) T(\eta)$$

$$\frac{\delta T}{T} \simeq -2y$$

$$\frac{\delta T}{T} = \sigma_T c \int d\eta n_e(\eta) v_e$$

- Two Different Effects
  - Thermal effect
    - Produces spectral distortion-- can be distinguished by multi-wavelength measurements
  - Kinetic Effect
    - Due to cluster motions

$$\int (\int nT ds) dA = \int p dV$$

Spectral Distortion

- Thermal SZ effect is the scattering of photons from low energy to high energy
- Detected in many clusters in pointed observations and may have been detected in unpointed surveys

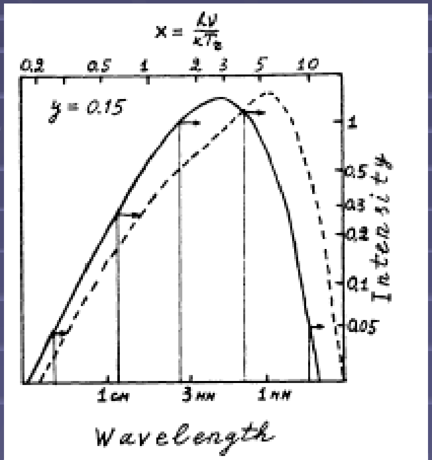

Sunyaev-Zeldovich 1980

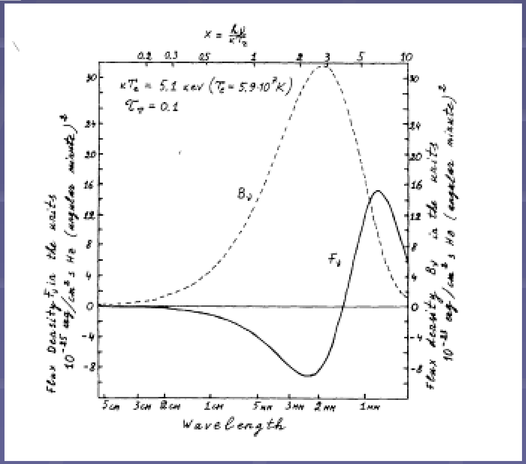

Komatsu Seljak 2002

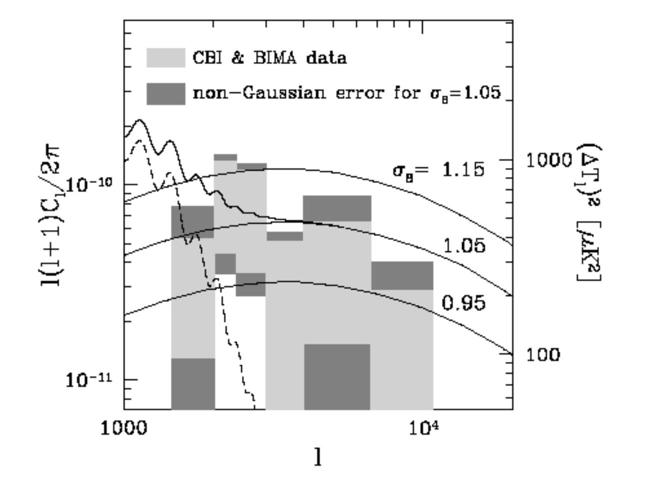

Figure 11. The CBI (Mason et al. 2002) and BIMA (Dawson et al. 2002) data with Gaussian errors (light-gray shaded area), the predicted SZ angular power spectra for $\sigma_8 = 0.95$, 1.05, and 1.15 (thin solid lines), the primary CMB anisotropy for the fiducial cosmological model (dashed line), and the sum of the two for $\sigma_8 = 1.05$ (thick solid line). The dark-shaded area gives non-Gaussian errors predicted for $\sigma_8 = 1.05$.

Sunyaev-Zel'dovich (SZ) clusters

Coma Cluster $T_{electron} = 10^8$ K

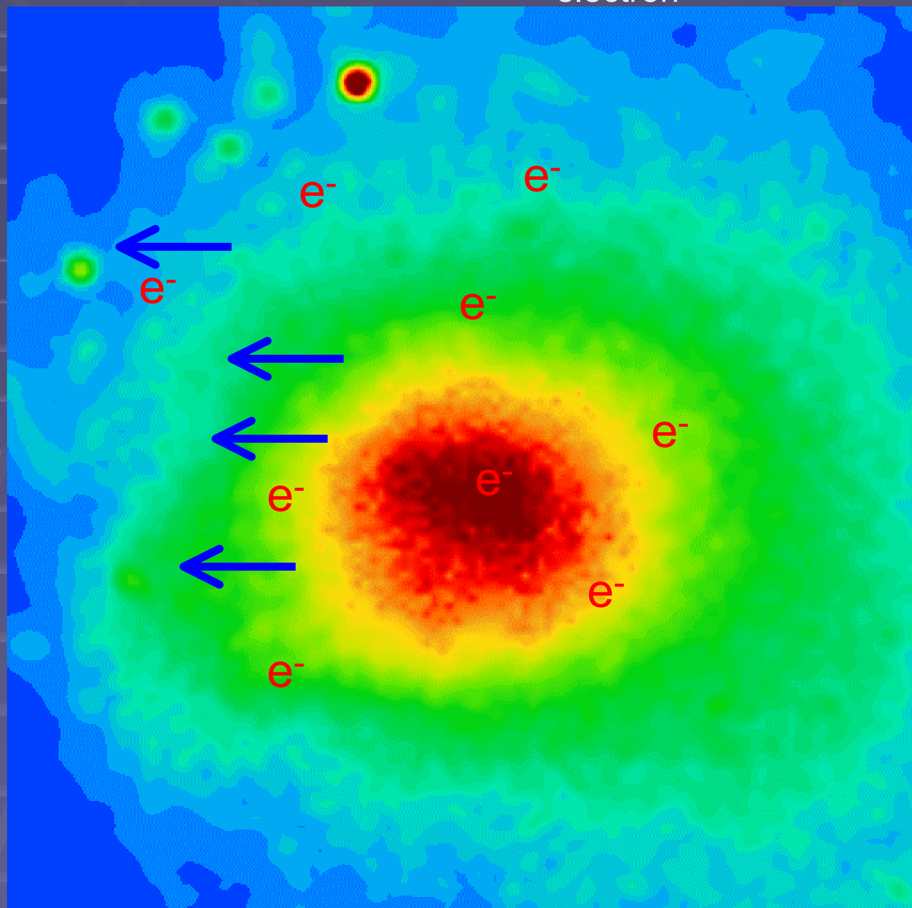

Optical:
Redshift and Mass

mm-Wave: SZ – Compton Scattering

X-ray Flux:
Mass

SZ Cluster Surveys

- Next generation CMB experiments will detect 1000s of clusters
- A thermal pressure selected surveys
- Very useful for astrophysics
- Use for cosmological tests is very sensitive to cluster SZ luminosity/mass conversion

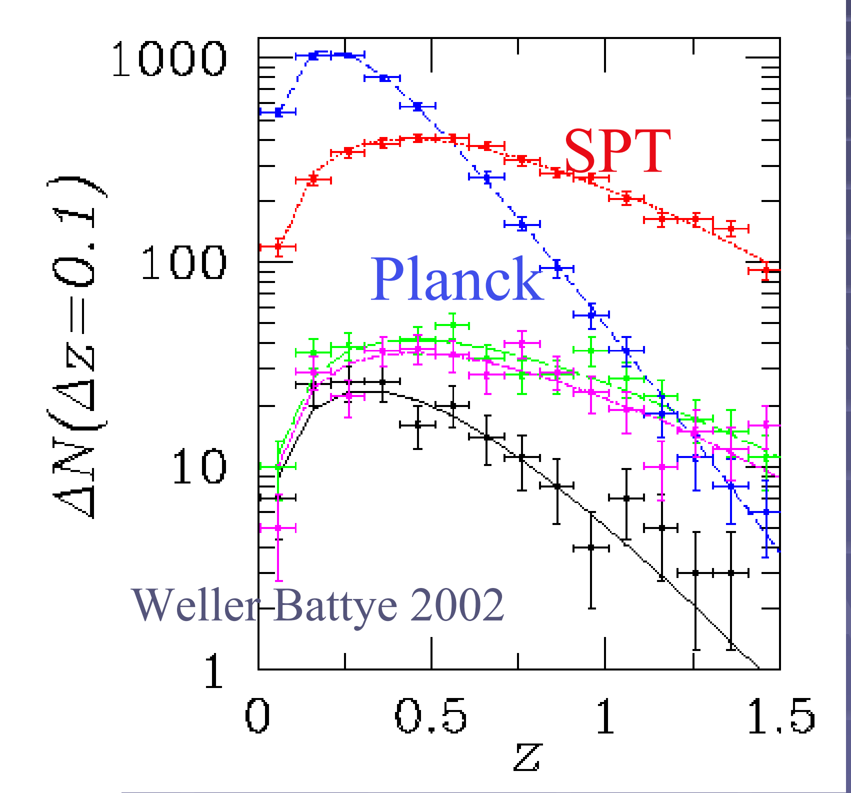

Dark energy properties

$$\frac{dN}{dz} = \Delta\Omega \frac{dV}{dz d\Omega}(z) \int_{M_{\lim}(z)}^{\infty} \frac{dn}{dM} dM \,,$$

Exponentially sensitive to $L_{sz}(M)$

Clusters are not simple thermalized clouds of gas

- Significant energy input from AGNs
- Non-thermal sources of pressure (cosmic rays, magnetic fields)
- Gas at virial radius is not likely in thermal equilibrium
  - Electrons and protons may not even be in thermal equilibrium

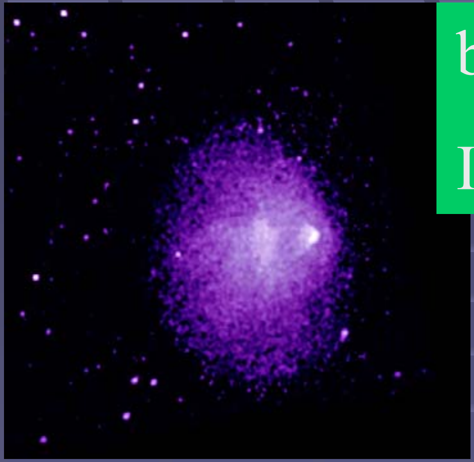

bow shock

IE0657-66

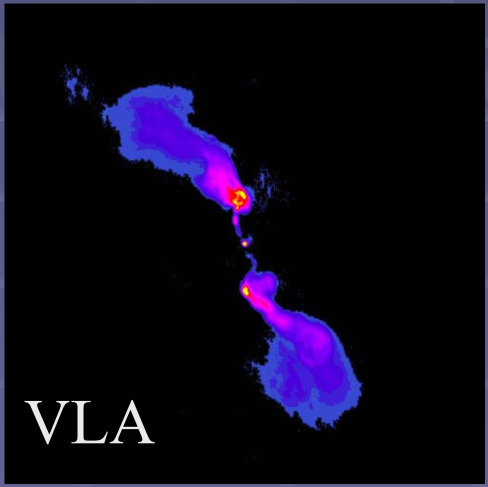

Hydra A

Doppler Effect Contribution

$$\frac{\delta T}{T} = \int d\eta n_e^0 [1 + \delta(\eta))] v(\eta) \sigma_T c$$

- Vanishes to linear order (except at the largest scales)
- Doesn't vanish to 2nd order (Ostriker-Vishniac effect)
- Inhomogeneous reionization leads to additional fluctuations

Kinetic SZ/Ostriker-Vishniac (OV)

$$\delta T \propto \langle n_e^2 \rangle^{1/2} \langle v_e^2 \rangle^{1/2}$$

Bulk *Velocity of hot electrons.*

Bulk velocity of *HOT electrons from ionization by the first stars (OV) or in clusters and filaments (KSZ).*

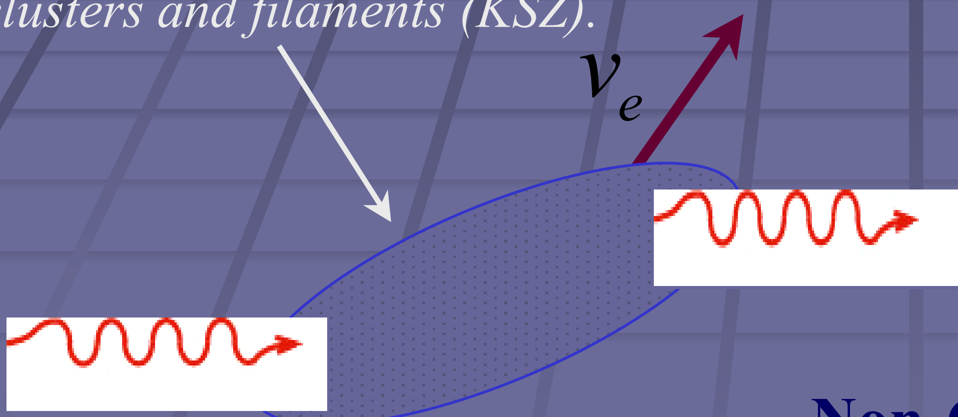

CMB photon

Amplitude of OV signal determines epoch of reionization.

OV power spectrum measures the density and velocity fluctuations at reionization.

KSZ measures cluster bulk velocity field at low z.

Non-Gaussian but with CMB frequency spectrum. Spatially distinguishable. Requires a high fidelity map.

Ostriker-Vishniac Effect

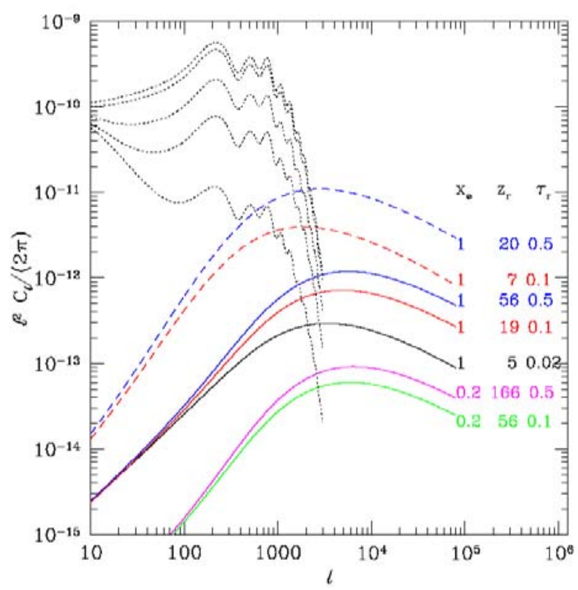

FIG. 1. Multipole moments for the Ostriker-Vishniac effect for the *COBE*-normalized canonical standard-CDM model ($\Omega = 1$, $h = 0.5$, $n = 1$, $\Omega_b h^2 = 0.0125$), for a variety of ionization histories, as listed. We also show predictions for several open high-baryon-density models with the same x_e and τ_r, normalized to the cluster abundance, with dashed curves. The dotted curves show the primary anisotropy for this model for $\tau_r = 0.0, 0.1, 0.5, 1$, and 2, from top to bottom.

- Amplitude very sensitive to reionization history
- Signal may correlate with LOFAR signal (should be investigated)

Kamionkowski & Jaffe 1998

ACT - Atacama Cosmology Telescope

- 6 Meter Aperture
- Low Ground Pickup (< 20μK dc)
- No Moving Optics
- Remote Controlled
- Flexible Focal Plane
- Near the ALMA Site

Concept Sketch

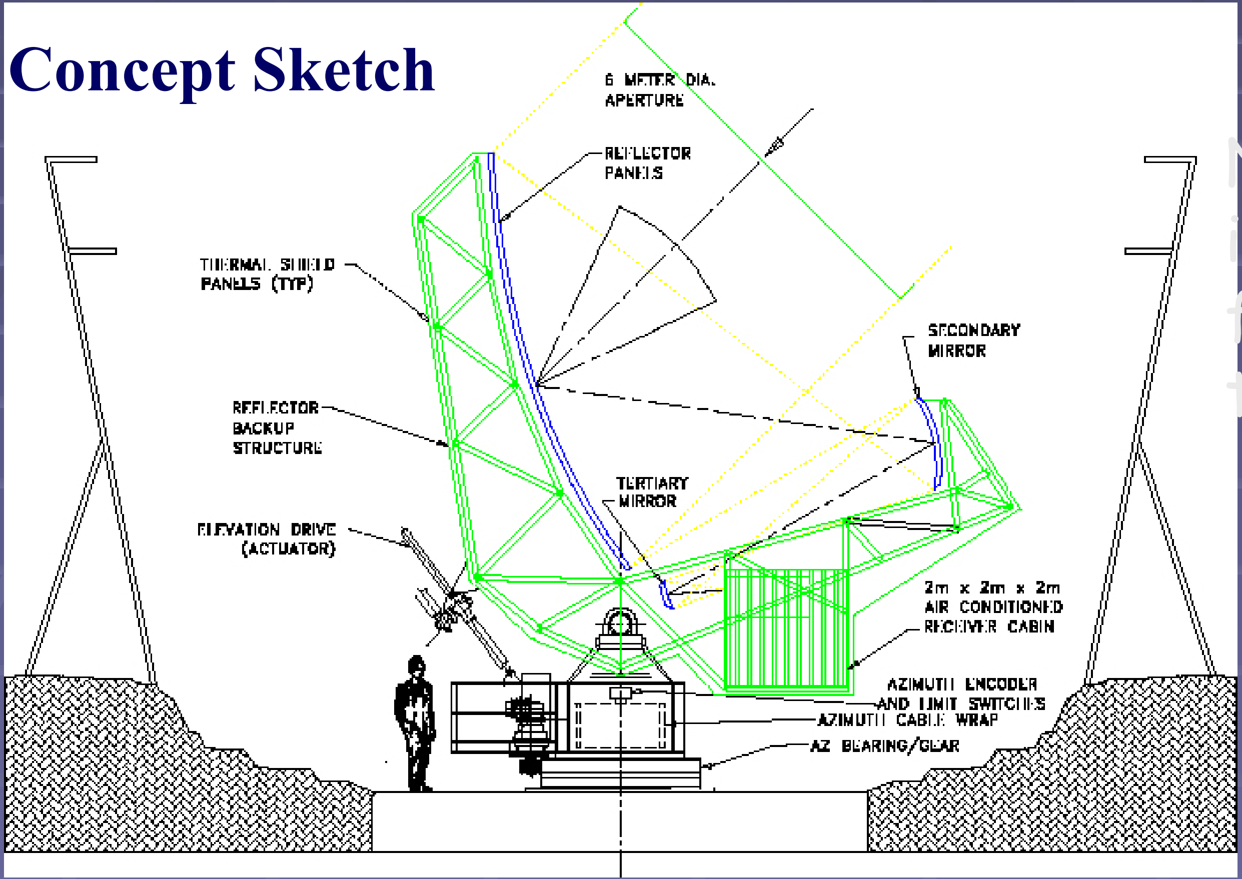

No existing telescope incorporates the features required for these measurements.

Extreme control of potential systematic errors.

Arcminute Resolution mm-wave Observations

150 GHz

1.4°

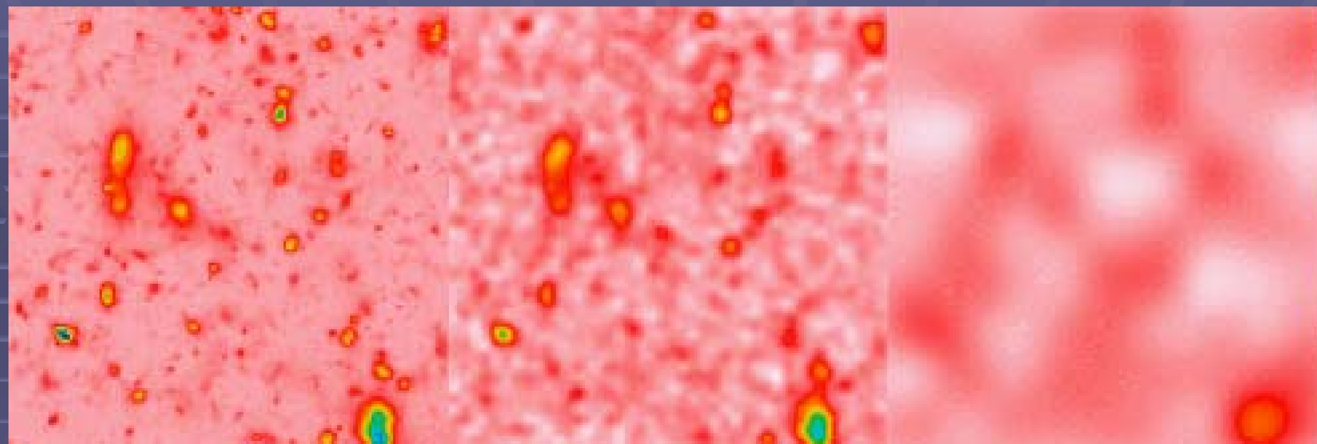

< 1% of survey area

~2% of high quality area

SZ Simulation **MBAC on ACT 1.7' beam w/ 2X noise** **PLANCK**

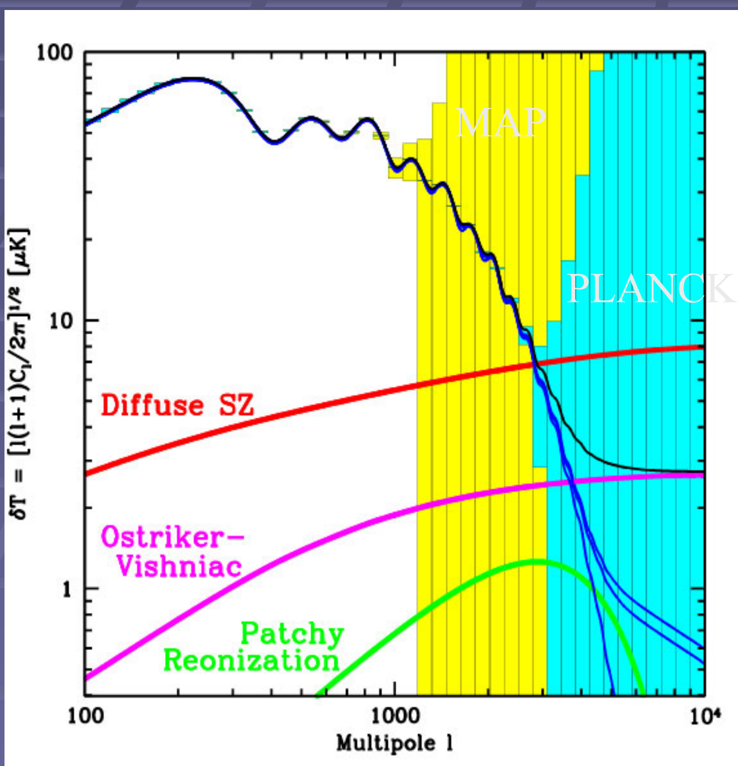

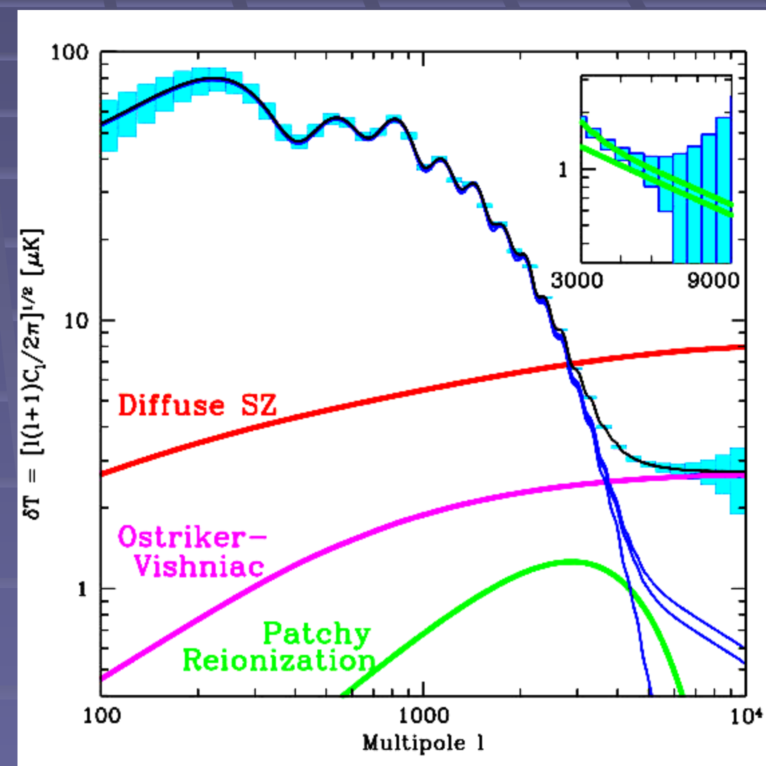

Why Atacama?

- 5200 meter elevation
- One of driest places on planet
- Gently sloping topography ⇒ low turbulence
- The future site for ALMA
- Logistical support available
- 24 hours travel from Center to Site!

Possibly the best millimeter observing site available

How to Get to ACT

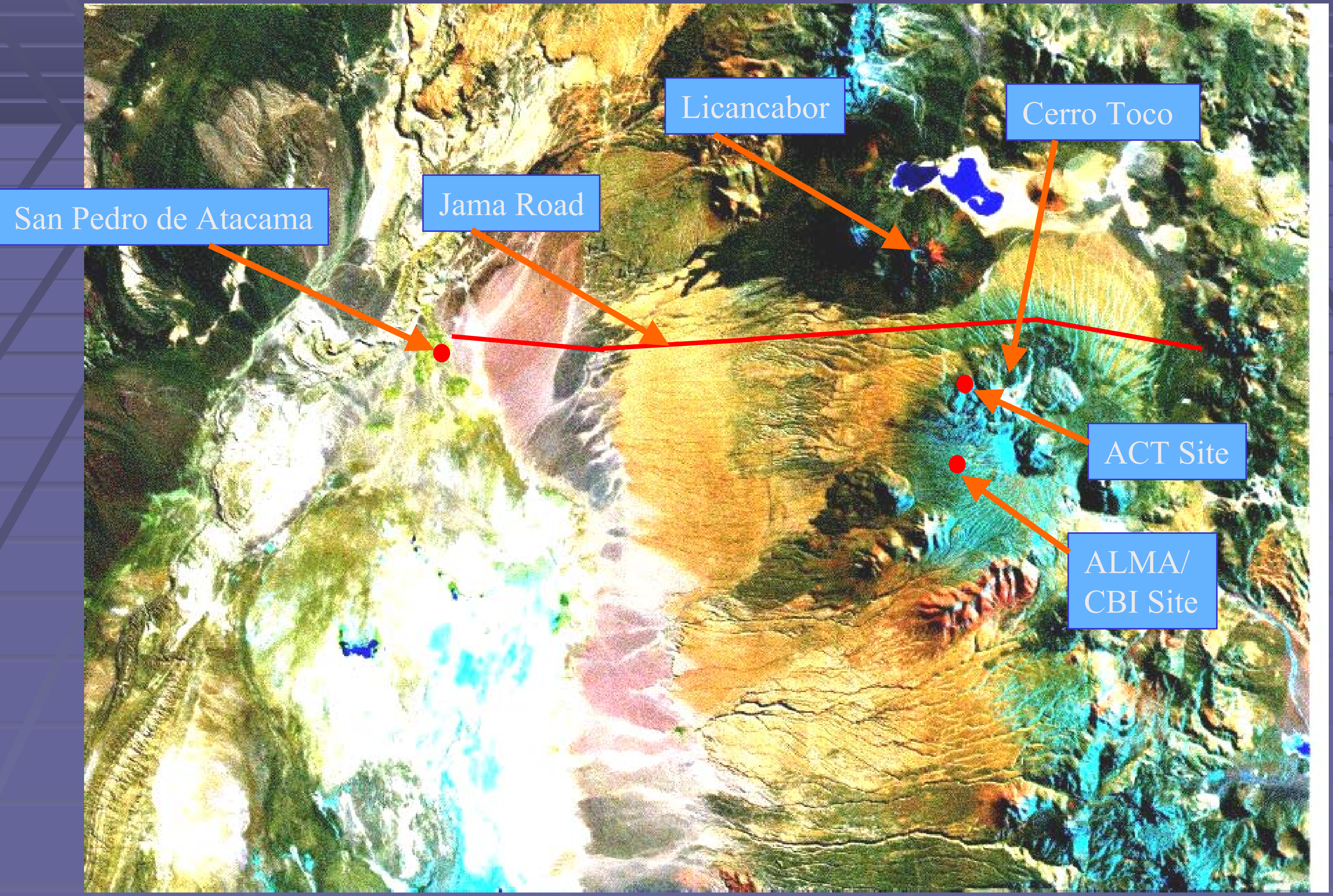

~100 km

Close-up View

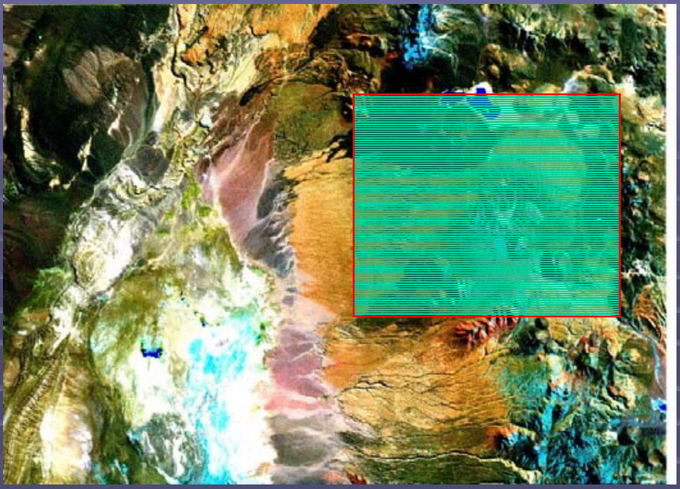

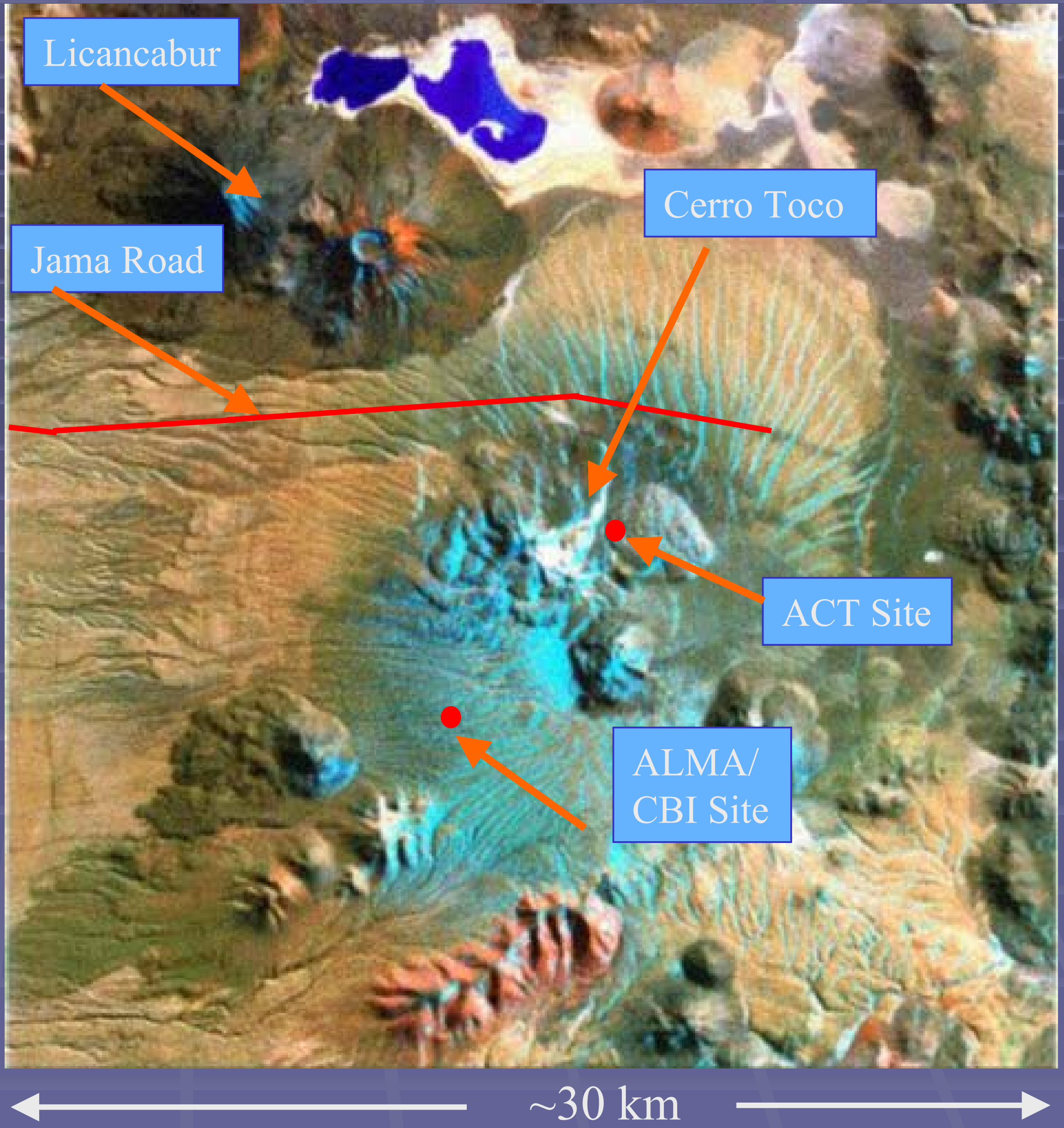

• The Jama road is a paved highway which is passable year-round.

• The ACT and CBI sites are accessible via mining roads off the Jama road.

• CBI is further from the Jama road than ACT and at a more windy site.

• It takes 50 min. to get from San Pedro to the ACT site.

• ACT is completely remote controlled. No overnight stays at the site.

145 GHz Maps

Map Components

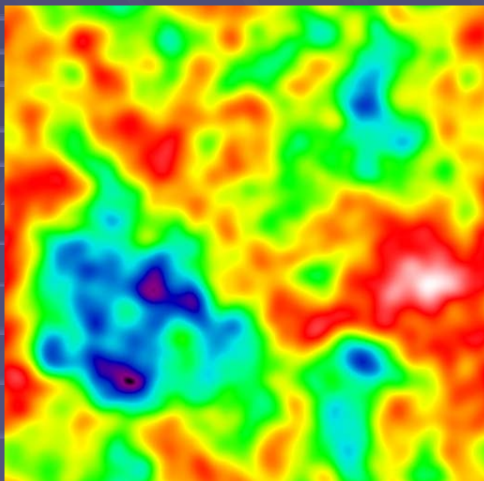

CMB

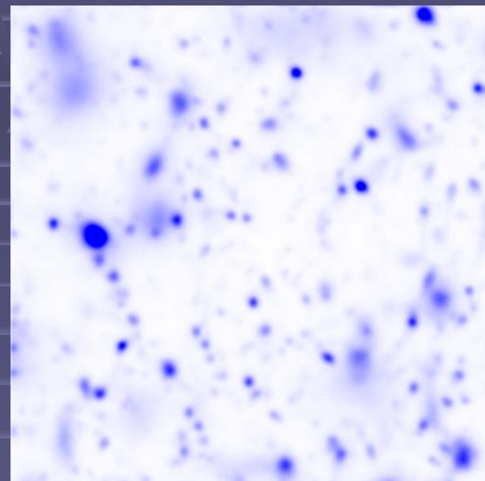

SZ

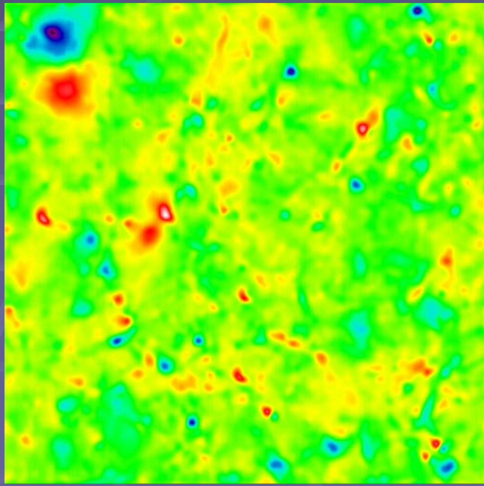

KSZ/OV

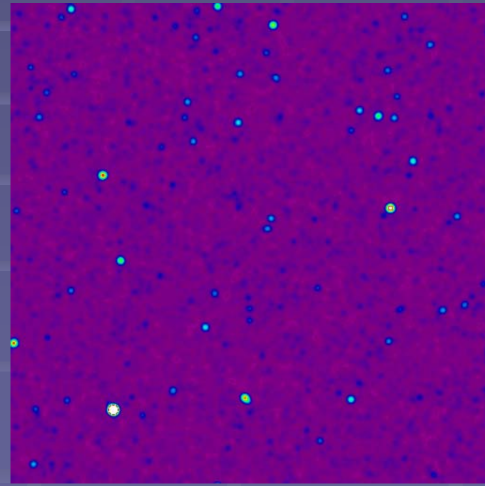

Point Sources

Components Summed to Scale

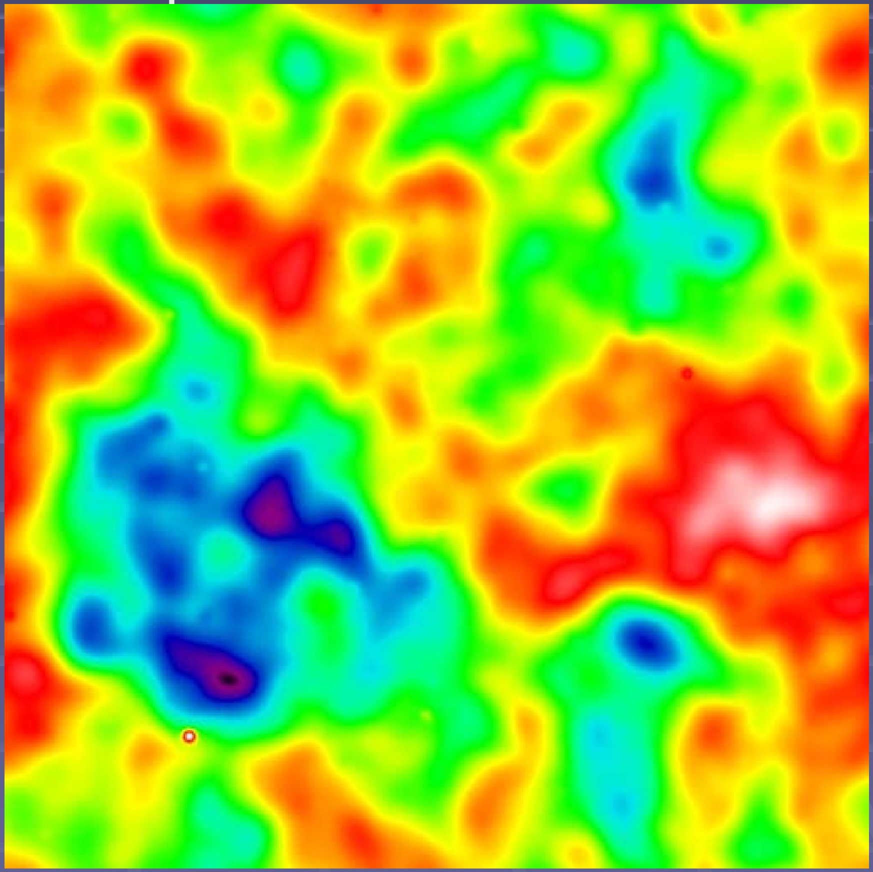

1.4°x 1.4°

220 GHz Maps

Map Components

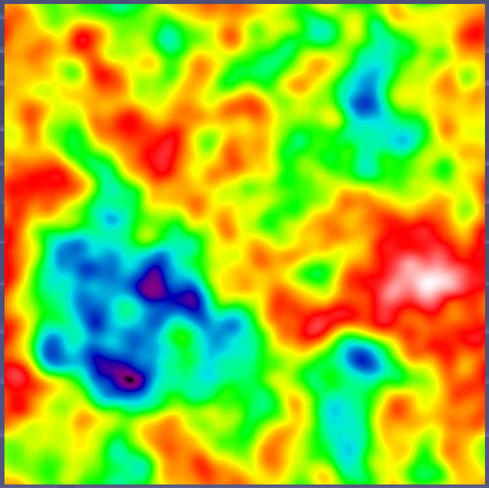

CMB

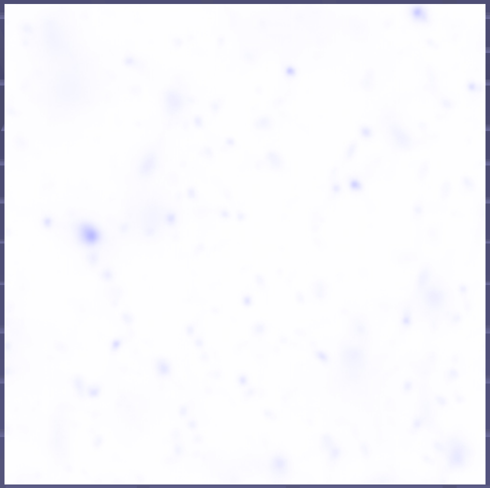

SZ

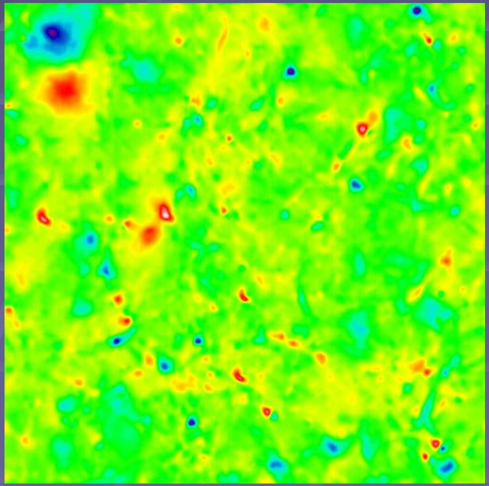

KSZ/OV

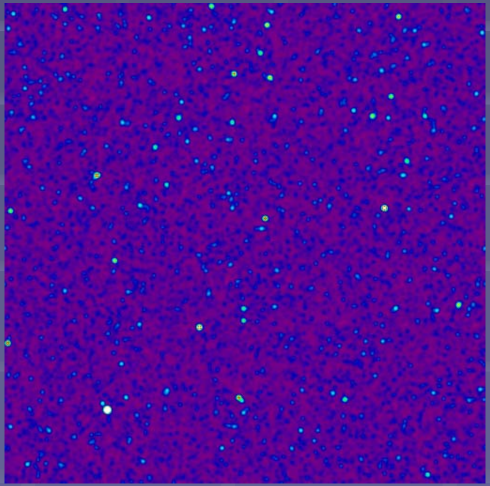

Point Sources

Components Summed to Scale

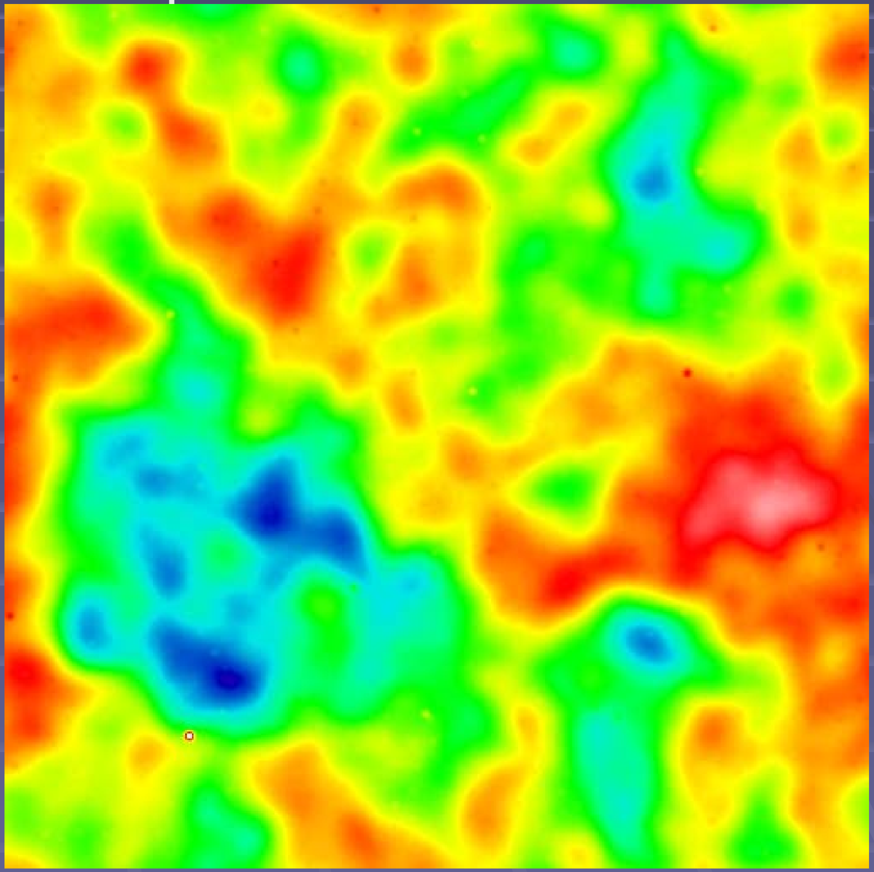

1.4°x 1.4°

270 GHz Maps

Map Components

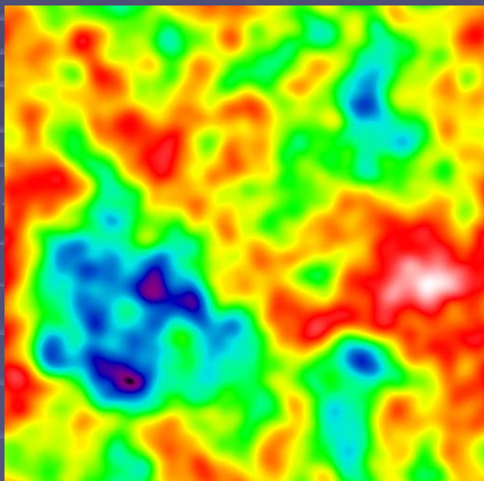

CMB

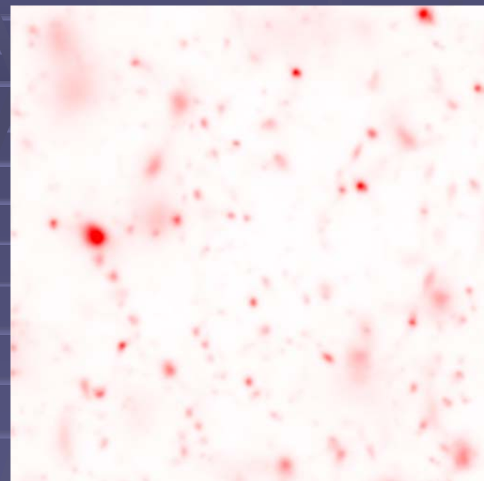

SZ

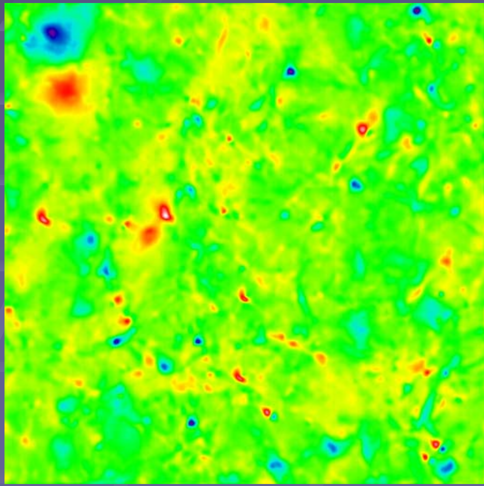

KSZ/OV

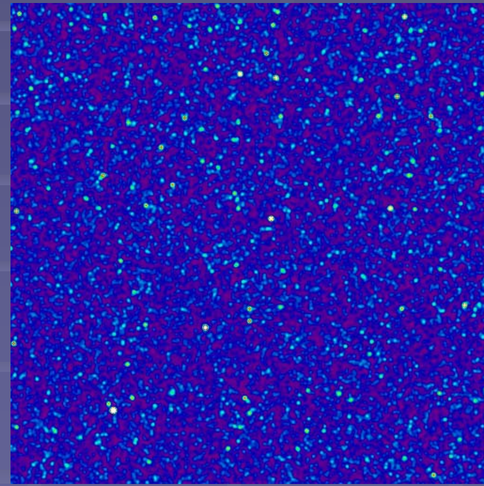

Point Sources

Components Summed to Scale

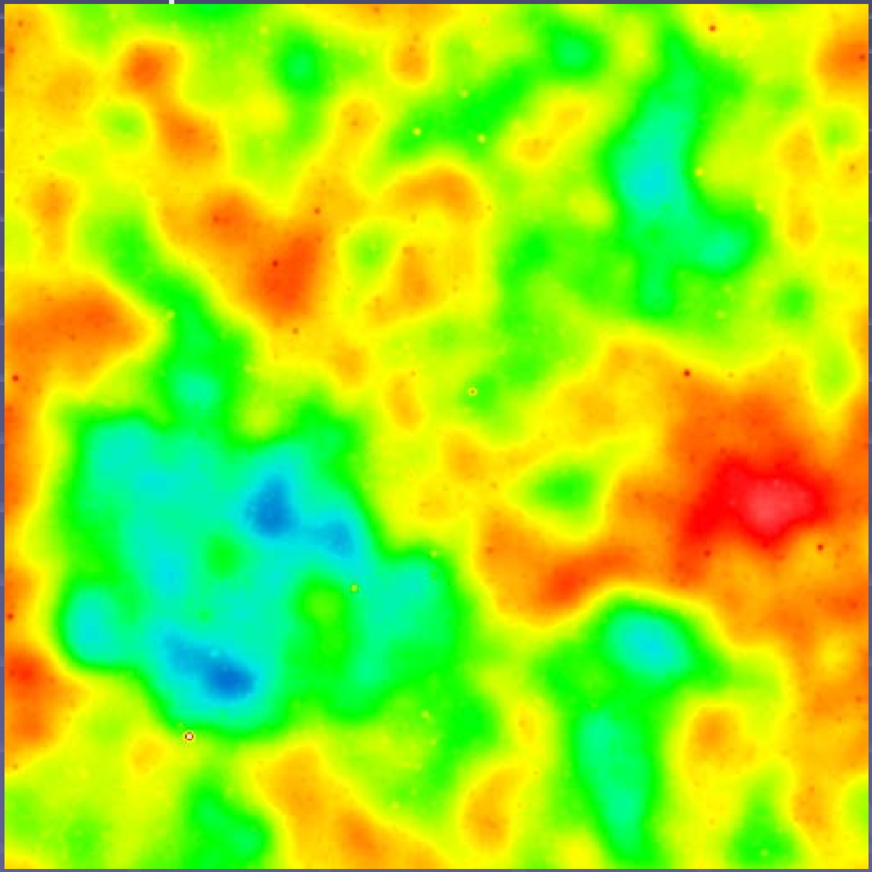

1.4°x 1.4°

Multiwavelength Studies

- Crosscorrelation of lensing signal
- Cluster properties
  - Xray
  - Optical
  - Radio
- Ionized universe
  - LOFAR and KSZ

Conclusions

- CMB observations will continue their dramatic improvement over the next decade
- Probe of both early universe physics and of the emergence of structure
  - Important complementarity with optical and X-ray measurements

Further Reading

- Peacock, John, Cosmological Physics
- Dodelson, Scott
  - Best for CMB fluctuations, linear theory}
- Liddle and Lyth, Inflationary Cosmology
- Peebles, Large Scale Structure (out of print)

How a TES Bolometer Works

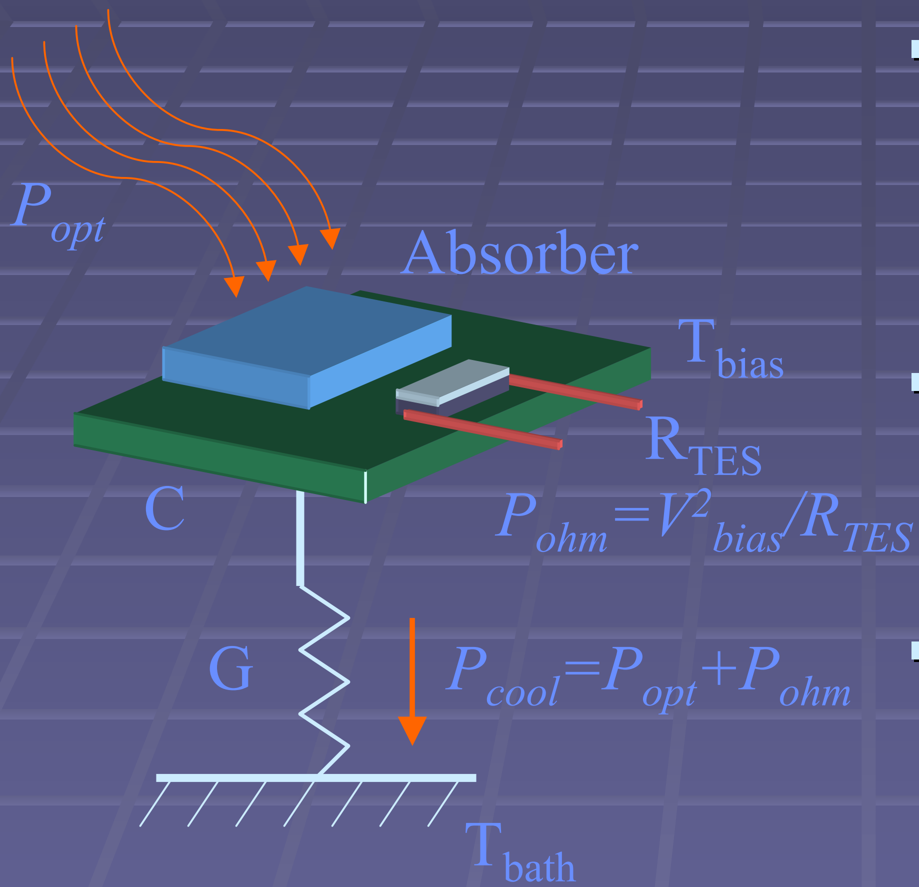

- TES Detector features good noise performance, high sensitivity, high speed, linear behavior, and few strange effects
- Superconducting bolometers have much simpler thermal interfaces than semiconducting bolometers
- Multiplexed readouts have been developed, permitting large arrays with simple electronics

Revolutionary Detector Technology: CCD-like Arrays of Bolometers

- Pop-Up Detector (PUD): flat, monolithically fabricated array is folded to produce a detector where the wiring is behind the active area
- HAWC/SHARC have demonstrated this approach

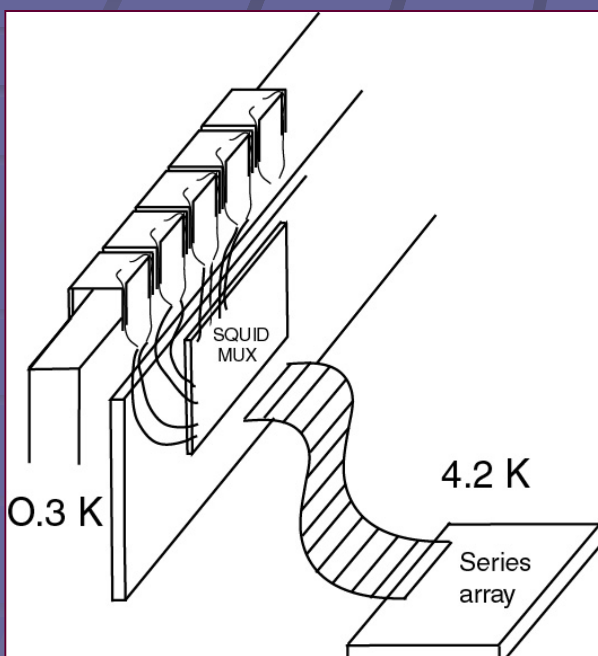

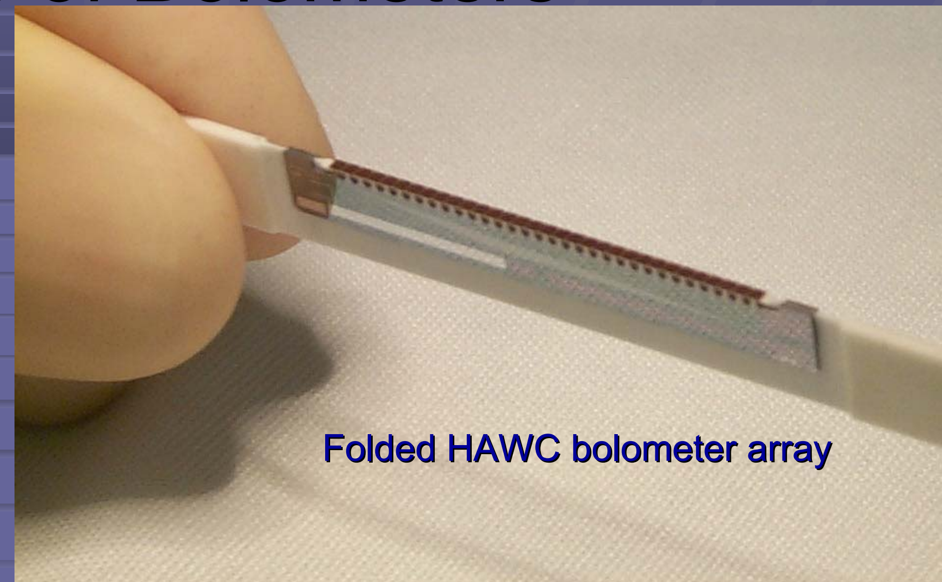

Folded HAWC bolometer array

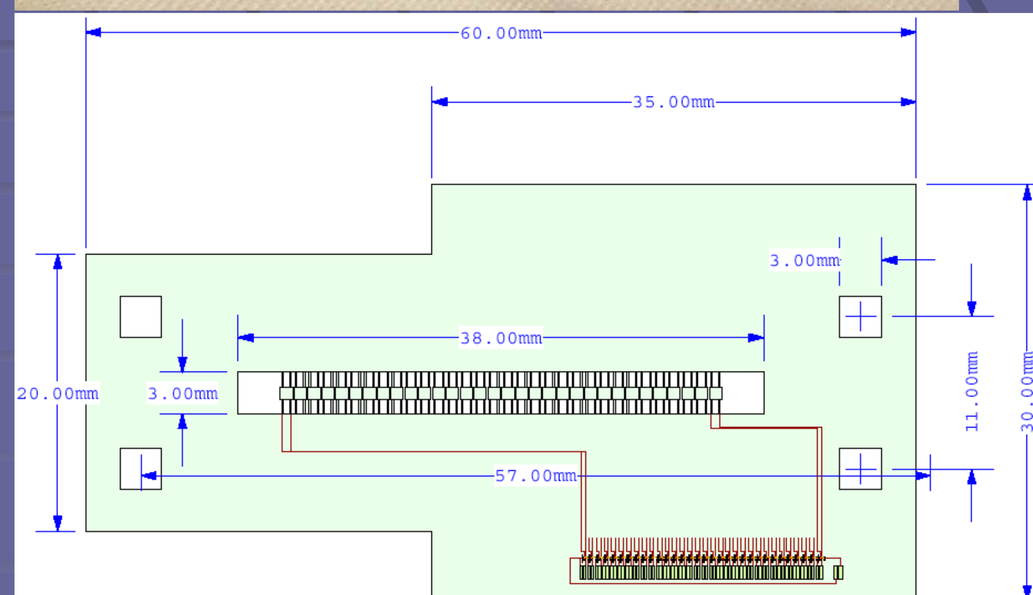

PUD layout for SAFIRE/SPIFI

Assembly

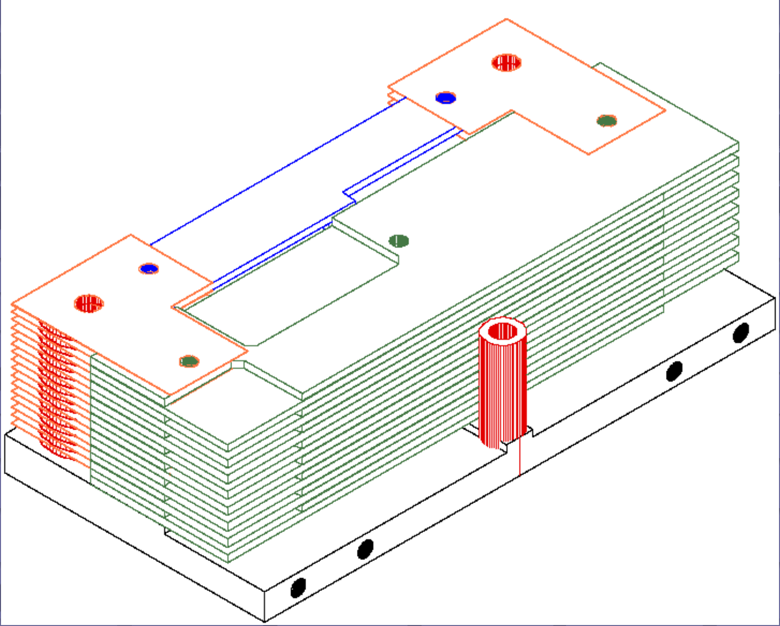

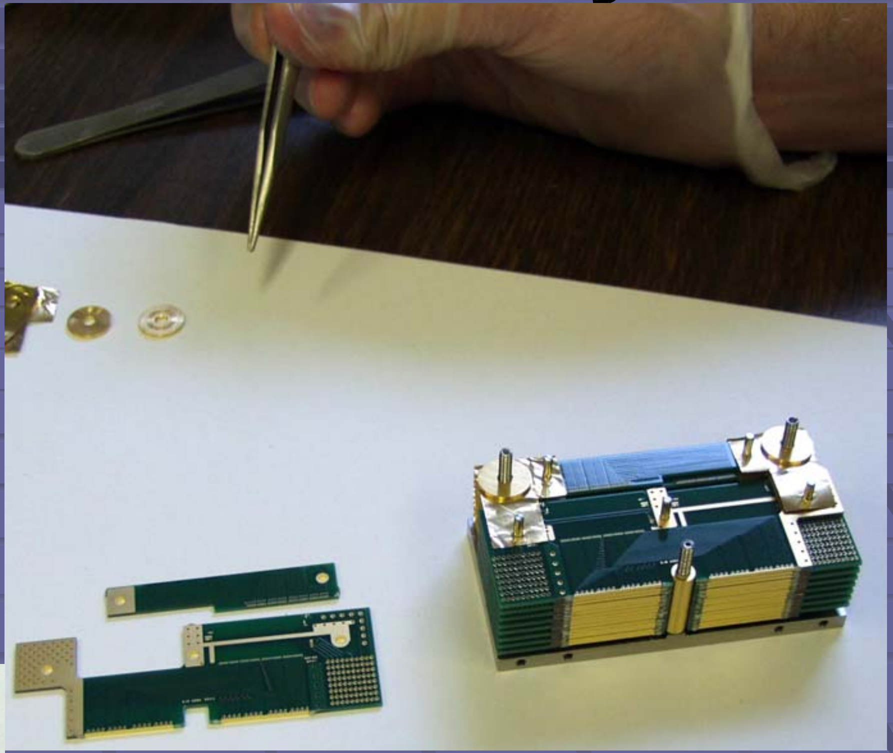

SAFIRE/SPIFI: Mechanical Prototype

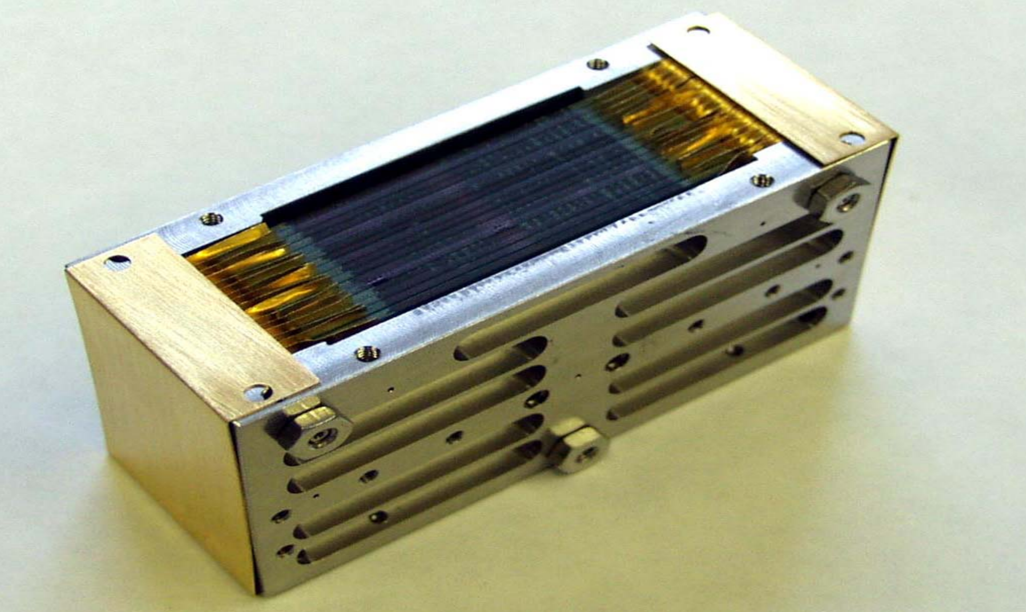

Realistic ACT Optical Design

- 6 m Primary, 2 m Secondary
- Modular 3 camera design
- Strehl Ratios > 0.95 across all fields at secondary and final foci

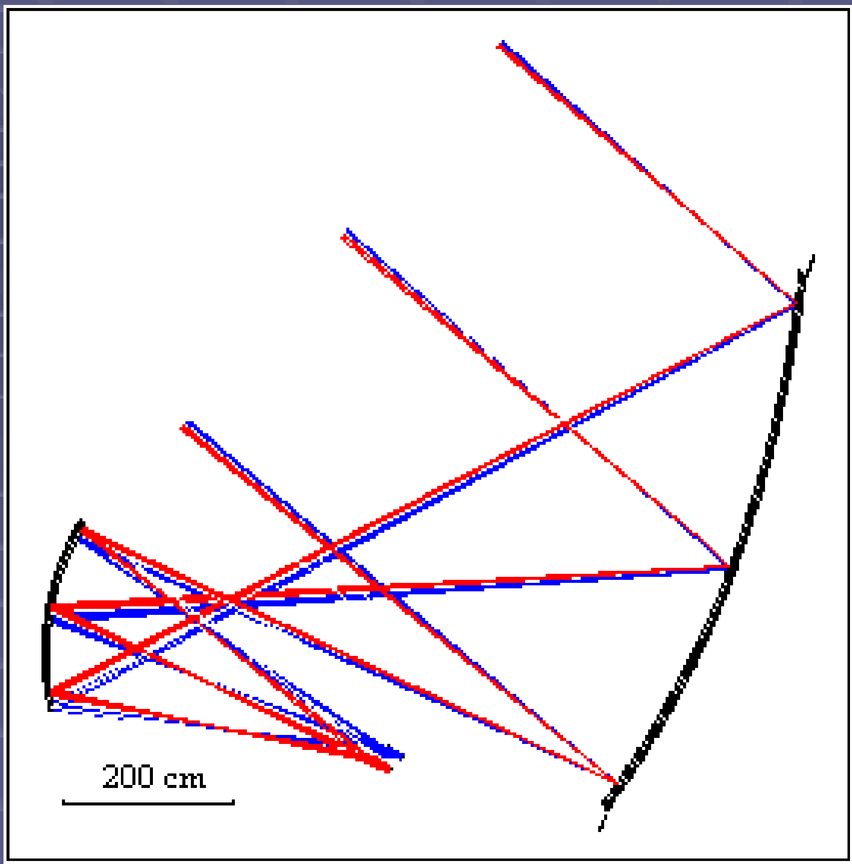

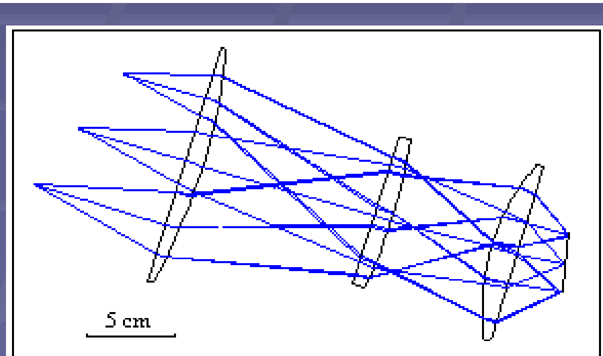

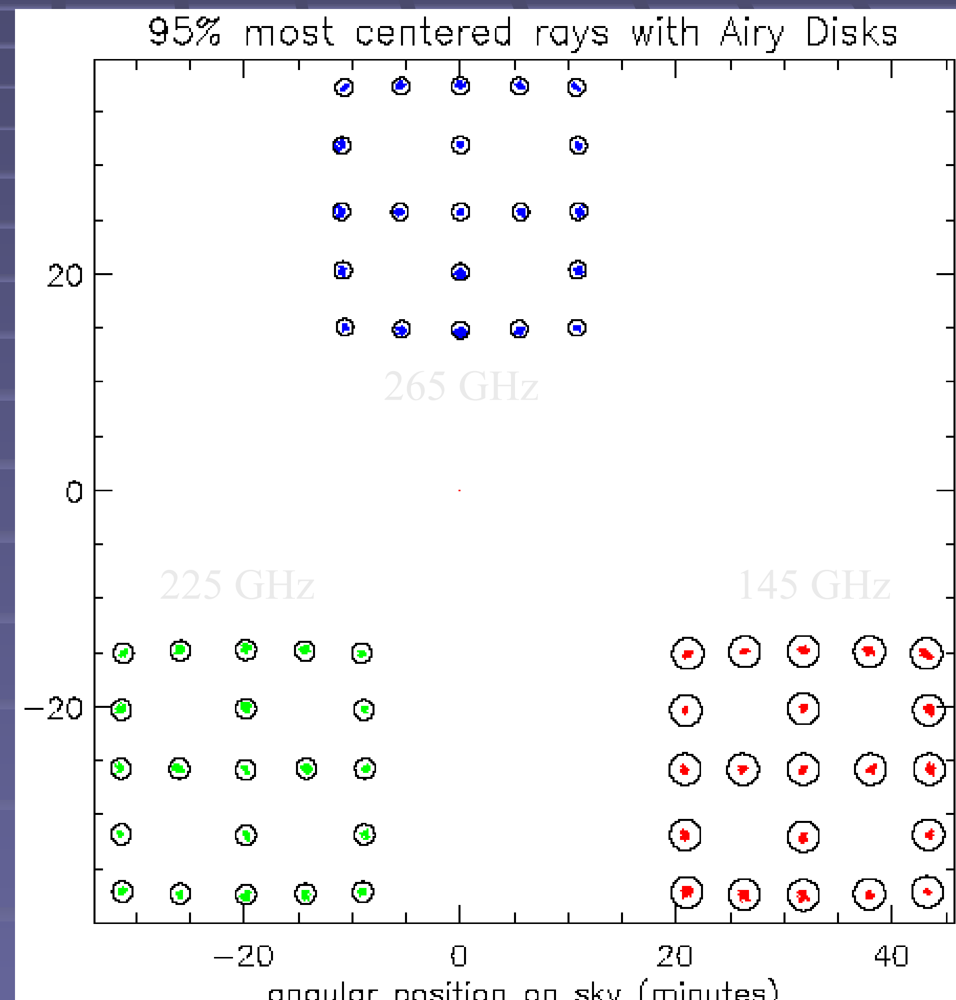

What Atmosphere?

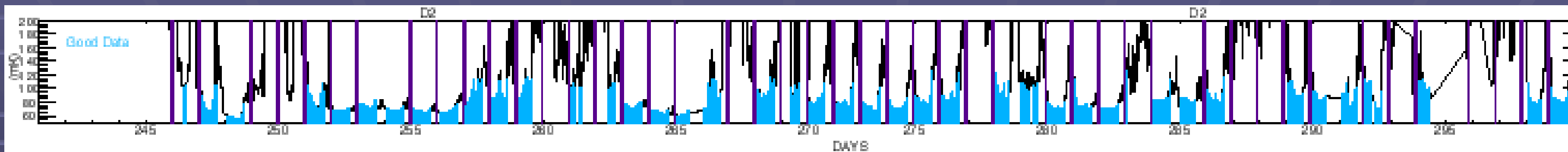

Measured: 65% of the nights exceed the most stringent requirements.

- Only 65 nights required

- The atmospheric noise is below instrument noise ($l > 600$)

- All of our critical science is at $l > 600$

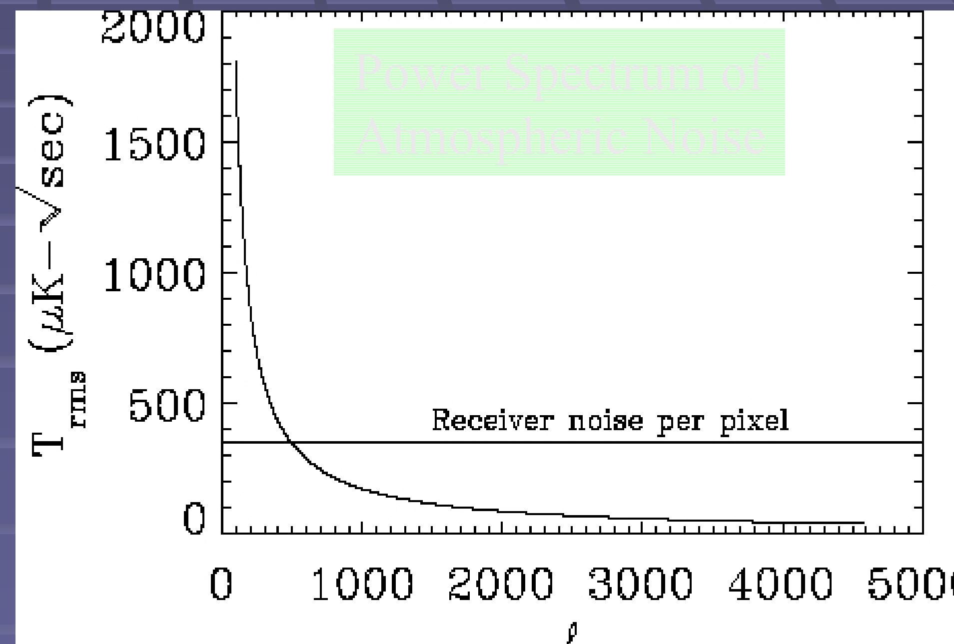

The atmosphere is essentially featureless for $l > 1000$.

(based on Lay & Halverson)

For $l < 1000$ solve for atmosphere with swept, over-sampled, filled array.

Cross Linked Scan Strategy is Crucial to Making Maps on Degree Angular Scales

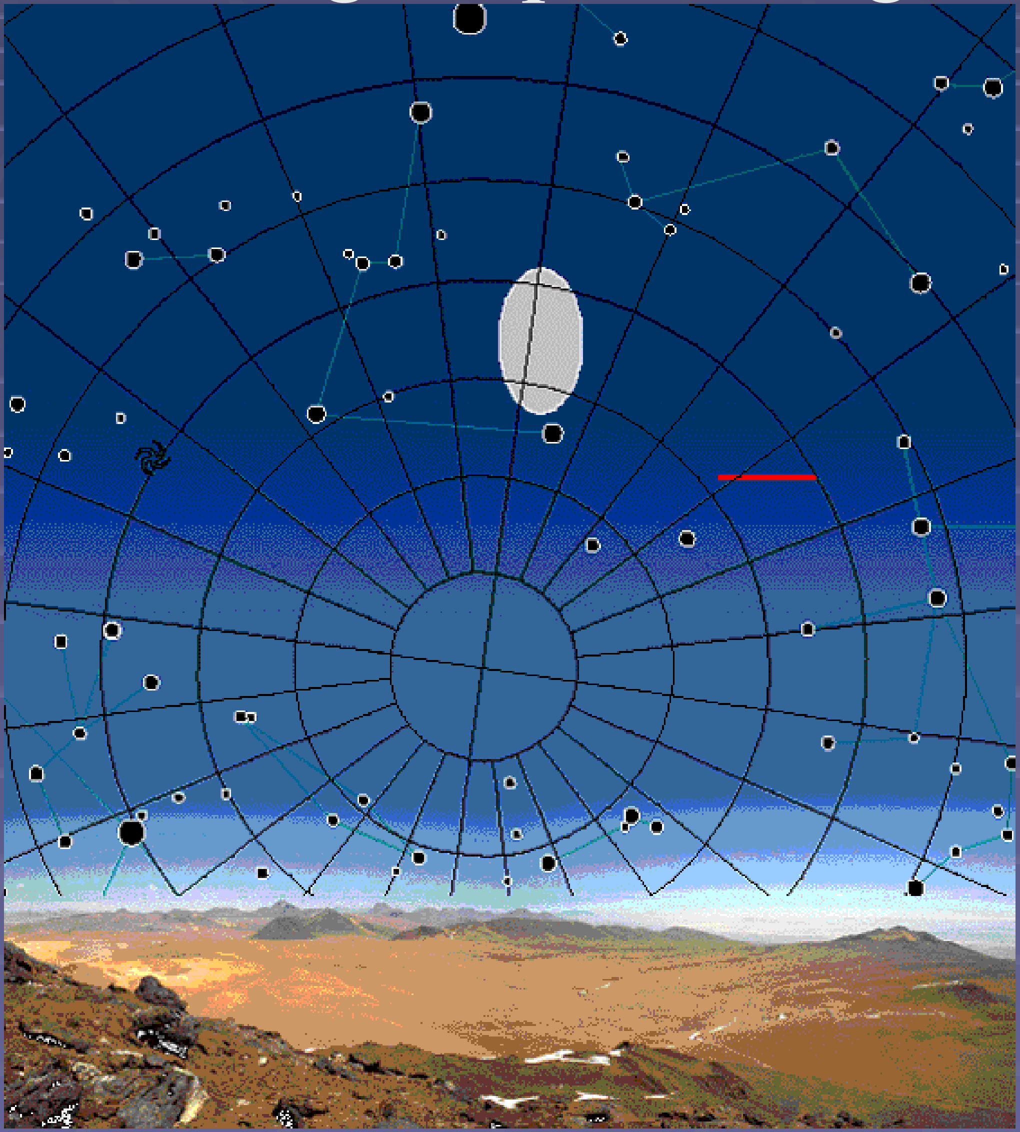

- 240 square degrees in circle
- 100 square degrees for CMB
- Connect to MAP satellite for calibration
- Rich Galactic data set

- Start work in January 2004
- First Light in November 2006
- Complete Observing December 2008

Sky Coverage

ACT's sky cover overlaps with that of Northern and Southern hemisphere telescopes.

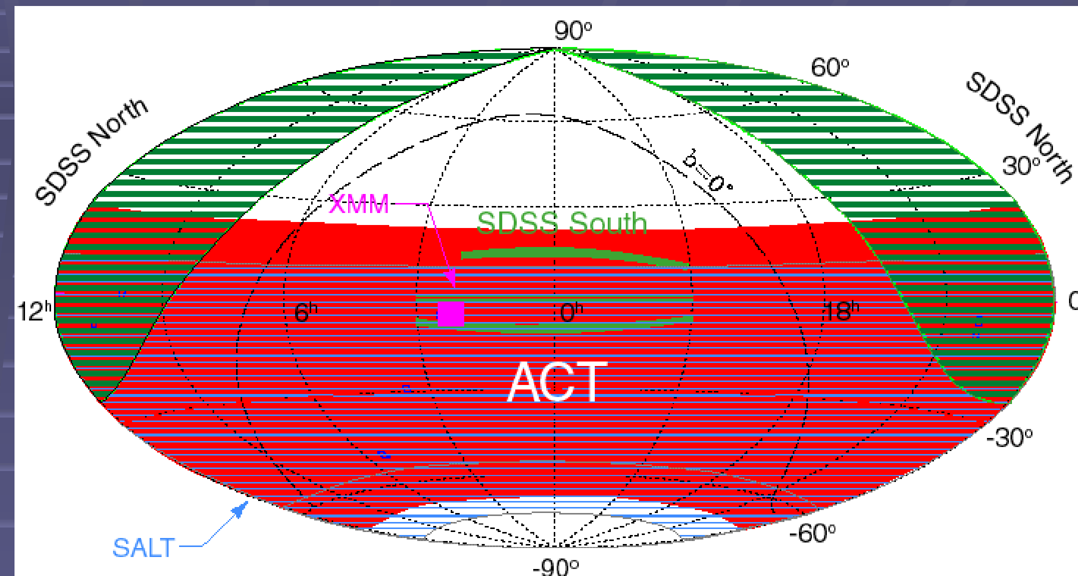

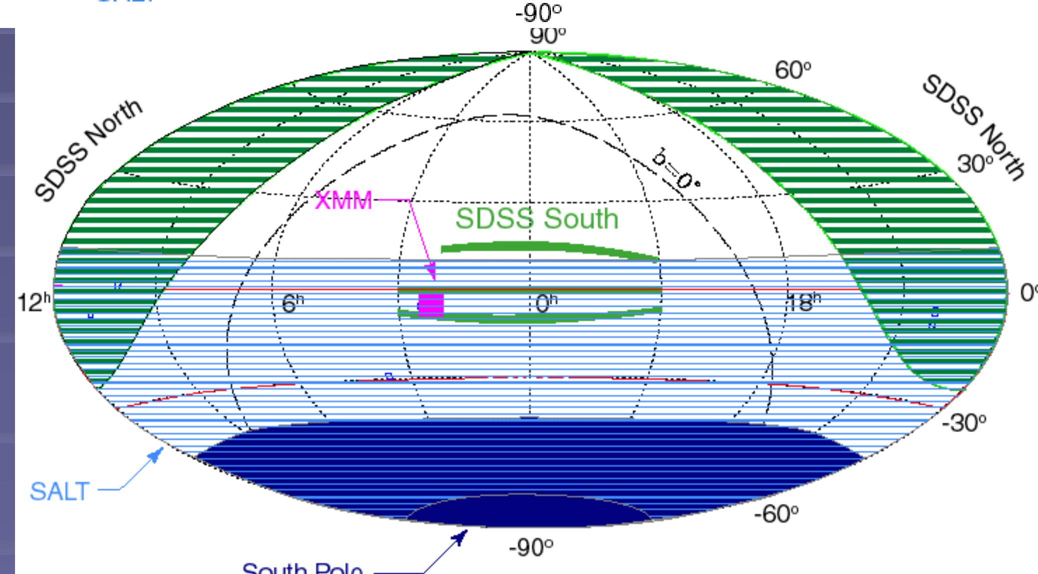

Technology